

The Air Cooled Condenser Optimization

by

Martin Squicciarini

B.S., Widener University, 2010

A REPORT

Submitted in partial fulfillment of the requirements for the degree

MASTER OF SCIENCE

Department of Mechanical and Nuclear Engineering
College of Engineering

KANSAS STATE UNIVERSITY
Manhattan, Kansas

2016

Approved by:

Major Professor
Dr. Donald L. Fenton

Copyright

© Martin Squicciarini 2016.

Abstract

Today air cooled chillers are often used in industrial applications where chilled water is pumped through processes or laboratory equipment. Industrial chillers are used for the controlled cooling of products, mechanisms and factory machinery in a wide range of industries. However, there is limited information on condenser coil design for a simulated model that uses R407c in a process chiller system with a focus on the finned tube condenser design. Therefore, a simulation tool that evaluates the performance of a condenser design, e.g. frontal area, cost, and overall system efficiency would be very useful.

An optimization calculator for the air cooled fin-tube condenser design was developed. This calculator allows a user to specifically select the condenser geometric design parameters including the overall condenser length and height, number of rows, number of circuits, row and tube spacing, fin thickness, fin density, tube inner and outer diameters, and the quantity and power of the fan motors. This study applied the calculator finding an optimum condenser design for various frontal areas and cost constraints. The calculator developed is appropriate for engineering designers for use in the process chiller industry.

Table of Contents

List of Figures	v
List of Tables	vi
Nomenclature	vii
List of Supplemental Files	xi
Acknowledgements.....	xii
Chapter 1 - Introduction.....	1
Chapter 2 - Background Chillers	5
Chapter 3 - Background Refrigeration Cycle	7
Chapter 4 - Chiller System and Component Modeling.....	11
Chapter 5 - Optimization Parameters.....	25
Chapter 6 - System Optimization.....	37
Chapter 7 - Conclusions and Recommendations	46
Chapter 8 - References.....	49

List of Figures

Figure 1: Size Comparison of Existing Chillers (Drake Refrigeration 2016)	4
Figure 2: Temperature vs. Entropy Diagram (D.G. Rich 2009)	8
Figure 3: Cross-flow Heat Exchanger (Bergman 479)	9
Figure 4: Actual Vapor Compression Refrigeration cycle (Jacobi 2006).....	9
Figure 5: Staggered Tube Arrangement in Bank of Condenser (AKAspelund 5).....	15
Figure 6: Staggered Tube Layout-Side View (Bergman 469).....	20
Figure 7: Friction Factor and Correction Factor for Staggered Tube Arrangement (Bergman 2011)	22
Figure 8: Effect of Operating Conditions on 70 in. x 36 in. Condenser	27
Figure 9: Saturated Condensing Temperature vs. Subcooling.....	29
Figure 10: EER vs. Subcooling.....	30
Figure 11: Common Chiller Assembly (Drake Refrigeration)	31
Figure 12: Saturated Condensing Temperature vs. Volumetric Airflow	32
Figure 13: EER vs. Volumetric Airflow	33
Figure 14: Staggered Tube Arrangement in a Bank (Bergman 2011)	34
Figure 15: Air Pressure Drop vs. Air Velocity	35
Figure 16: Air Leaving Temperature vs. Air Velocity	36
Figure 17: Overhead View of PAC180D (Drake Refrigeration)	38
Figure 18: Fan Curve (Drake Refrigeration)	39
Figure 19: Air Pressure Drop vs. Rows	41
Figure 20: Saturated Condensing Temperature vs. Rows.....	42
Figure 21: EER vs. Rows.....	43
Figure 22: Yearly Operating Cost vs. Rows	43

List of Tables

Table 1: C2 Correction Factor Table (Bergman 2011).....	21
Table 2: Baseline Condenser Characteristics.....	26
Table 3: Simulated Condenser Sizes.....	28

Nomenclature

Variable	Name	Units
A	Heat transfer area	In ²
A _c	Cross sectional area of tubes	In ²
A _{fin}	Total fin surface area	In ²
A _{fr}	Frontal area of the Condenser	In ²
A ₀	Total air side heat transfer area including the fin and tube area	In ²
C _p	Specific heat at constant pressure	Btu/lb-F
C _{max}	Maximum heat capacity between that of air and the refrigerant	Btu/lb-F
C _{min}	Minimum heat capacity between that of air and the refrigerant	Btu/lb-F
C _{ratio}	Ratio of Cmin to Cmax	---
COP	Coefficient of Performance	--
C ₁	Constants of equation for a tube bank in cross-flow with a staggered configuration	--
C ₂	Correction factor for a bank of tubes with less than 20 rows	--
D, d	Tube Diameter	In
dpdLr	Pressure drop per unit length	Psi/in
EER	Energy Efficiency rating	--
f _{liq}	Friction factor or liquid	--
f _{vap}	Friction factor or vapor refrigerant	--
Gr	Total mass flux	Lb/(in ² -s)
H	Condenser height	In

h_1	Specific enthalpy of refrigerant entering the compressor.	Btu/lb
h_2	Actual specific enthalpy of refrigerant exiting the compressor	Btu/lb
h_3'	Specific enthalpy of refrigerant exiting the superheated portion of the compressor.	Btu/lb
h_3	Specific enthalpy of refrigerant entering the sub-cooled portion of the compressor.	Btu/lb
h_4	Specific enthalpy of refrigerant entering the expansion valve.	Btu/lb
h_5	Specific enthalpy of refrigerant exiting the expansion valve.	Btu/lb
K	Thermal conductivity	Btu/(hr-ft-F)
K_f	Fin Thermal Conductivity	Btu/(hr-ft-F)
K_t	Condenser tube conductivity	Btu/(hr-ft-F)
L	Length of Condenser	In
LL	Condenser fin length	In
$L_{con,SC}$	Tube length of subcooled portion of condenser tubes	In
$L_{con,sH}$	Tube length of superheated portion of condenser tubes	In
$L_{con,sat}$	Tube length of saturated portion of condenser tubes	In
L_{tot}	Total length of condenser tubes	In
\dot{m}	Refrigerant mass flow rate through the compressor	Lb/s
mm	Extended surface parameter	--
N_L	Number of rows in a condenser coil	--
NTU	Number of Transfer units	--
N_T	Number of tubes per row	--

Nu	Nusselt Number	--
Pe	Perimeter	In
Pr	Prandtl Number	--
\dot{Q}	Rate of total heat transfer between the refrigerant and the air	Btu/hr
$q_{con,sat}$	Amount of heat per unit mass transferred between the air and the refrigerant in the saturated portion of the condenser	Btu
$q_{con,sc}$	Amount of heat per unit mass transferred between the air and the refrigerant in the subcooled portion of the condenser	Btu
$q_{con,sh}$	Amount of heat per unit mass transferred between the air and the refrigerant in the superheated portion of the condenser	Btu
Q_{max}	Maximum possible amount of heat transferred between the refrigerant and air	Btu
r_o	Outer radius of condenser tube	In
r_{in}	Inner radius of condenser tube	In
Re	Reynolds number	--
r_{eq}	Equivalent radius for a hexagonal fin	In
R_w	Tube wall thermal resistance	(Ft ² -F-hr)/btu
sl	Longitudinal pitch	In
st	Transverse pitch	In
St	Stanton number	--
T_{ci}	Temperature of cold fluid entering the condenser	F
T_{hi}	Temperature of hot fluid entering the condenser	F
T_i	Inlet air temperature	F
T_o	Outlet air temperature	F

T_s	Condenser tube surface temperature	F
UA	Overall heat transfer coefficient	Btu/h
W	Condenser width	In
W_f	Condenser fan power	Watts
V	Velocity of air flowing over the condenser	Ft/s
FPI	Condenser fins per inch	#
X	Correction factor for condenser tube spacing and Reynolds number	--
X_l	Longitudinal tube spacing	In
X_t	Transverse tube spacing (normal to air flow)	In
ΔP	Pressure drop	Psi
ϵ	Fin effectiveness	%
ϕ	Fin parameter that is a function of the equivalent circular radius of a hexagonal fin	In
η_c	Compressor thermal efficiency	%
η_f	Fin efficiency	%
η_s	Surface Efficiency	%
η_{sa}	Air side surface efficiency	%
η_{sr}	Refrigerant side surface efficiency	%
μ	Viscosity	cp
ρ	Density	Lb/ft ³
ψ	Coefficient of the empirical relation for determining the equivalent circular radius for hexagonal fins.	--
v	Kinematic viscosity	Ft ² /h

List of Supplemental Files

1. “Calculator.xls”-Air cooled condenser simulator

Acknowledgements

I would like to acknowledge the support from John Kurish, General Manager of Drake Refrigeration, for his emotional and financial support of this project. It was through him that I was able to conceive and pitch my project idea and get approval to do this outside project. I would also like to gratefully acknowledge the leadership of Dr. Fenton in guiding me throughout this project and for his ability to bounce ideas off of. I would also like to thank my graduation committee including: Dr. Amy Betz and Dr. Shannin Nayyeri. Finally I would also like to thank Sankar Padhmanabhan, System simulation/Application Specialist with Danfoss, for sharing his knowledge on this topic. Sankar was able to answer all of my questions and was able to act as a great sounding board when discussing the goals of my project. I would most importantly like to thank my wife, Sarah, for her love and support while putting up with my early mornings and late nights working on this report.

Chapter 1 - Introduction

The selection of this project came from my experience in the refrigeration field since entering the work force seven years ago. I currently work for a chiller manufacturer, Drake Refrigeration, located in Bensalem, PA that specializes in custom design chillers to meet each customer's needs. Most chillers that are designed and then manufactured at our facility come requested with custom features based on the customer's wants, spatial restrictions, or specification restrictions. Drake Refrigeration specializes in doing single order projects for these custom units with quick turn around deliveries. Our product range includes air-cooled and water-cooled chillers that range from ¼ ton to 200 tons.

Through my time at Drake, I have come to realize that we did not have an accurate and cost effective way to simulate the smaller air cooled condensers. The system simulation software that came from the condenser manufacturer was very restrictive and limited in selection. We needed a way to quickly simulate a condenser coil that was not part of the standard product line that would allow us to get instant feedback. A system simulation is a mathematical calculation done in a software program that allows a user to input data and to generate results on how the system would operate based on these inputs. Depending on the software program this can include: system capacity, heat rejected, energy efficiency ratings, etc. By being able to make small changes to the condenser in a system simulation it would save thousands of dollars from testing the adjusted system in laboratory efficiency tests. The system simulator, that was produced for this project allows a user to input the desired condenser and compressor information and then output information on the system operation. This calculator is only going to do the calculations based on the inputs and a person familiar with refrigeration would need to interpret if this is a properly selected system. However, for an engineer attempting to conceptualize a custom chiller, being able to provide instant feedback is invaluable. This calculator will save Drake the time and money required to get every unit tested at a testing facility. When comparing this calculator to other simulators and laboratory results, it is able to produce results that are within 3-5% of actual results. This type of accuracy will allow Drake to use this program as a first pass alternative rating method when designing units. Now when a customer has a specific request, this calculator will allow an engineer the freedom to see how far the chillers can be adjusted and still achieve a desired result.

Using this simulator, I will specifically focus on a nominal 12.5 ton refrigeration circuit with the heat being removed by an air cooled condenser and fan(s). I will start with this chiller capacity and then build out the calculator to be used for other chiller systems. The reason for focusing on this size chiller is due to the high customer demand for this chiller in a compact design and the appearance of a gap in our product offering. Our current offering around this capacity includes an 8-ton single circuit, an 11-ton dual circuit, and 16-ton dual circuit model chillers that left a void in our chiller availability. This single circuit, 12.5-ton chiller will be able to fill this void along with being able to be sold at a lower price point than the dual circuit chillers. This is possible by using one refrigeration circuit to make it competitive in the market. We currently offer this 11-ton single refrigerant circuit chiller now with a larger and more expensive horizontal condenser assembly as shown in the picture on the top (PAC180S) of Figure 1: “Size Comparison of Existing Chillers”. The chiller has dimensions of 12 ft long x 3.75 ft wide x 5 ft high and has often caused spatial restrictions and problems for end customers. The cost from the horizontal condenser assembly and physical size of this unit are the main causes that have not allowed this chiller to be successful in the market. The lower picture (PAC180D) of Figure 1 is a 15 ton dual refrigerant circuit chiller with the dimensions of 7 ft long x 3.5 ft wide x 4 ft high. From Figure 1 below, the smaller footprint chiller, PAC180D is the size and style that we would like to design the new chiller based from. By being able to offer a compact single circuit 12.5-ton chiller, Drake will be able to bring down our cost per ton in this highly competitive process chiller market.

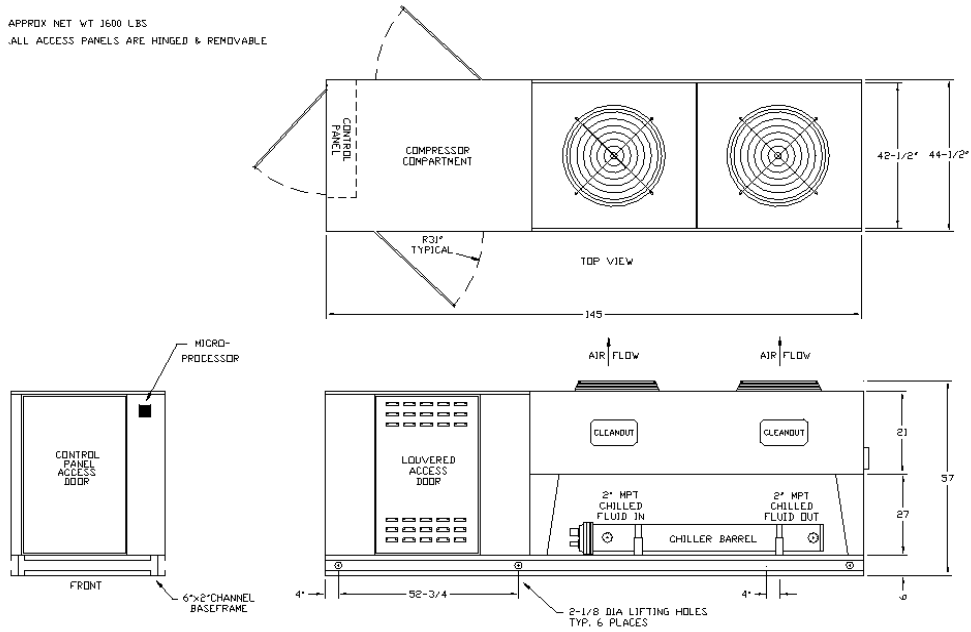
The goal of this project was to develop an air cooled condenser simulator or “calculator” that would allow for quick performance estimates and instant feedback. While, these are not certified laboratory results, they can help narrow down the number of tests to obtain an improved design prior to conducting expensive tests. I focused on one particular chiller model to simulate the required condenser and have already begun using this calculator for other existing chiller models. This in turn will lead to an efficient, expansion of the product offering. This calculator is able provide results for not only the condenser sizing but also a system analysis. This includes information related to the refrigerant circuit including compressor capacity, compressor discharge temperature, condenser total heat of rejection capacity, saturated condensing temperature, and refrigerant pressure drop through the condenser. This calculator can also provide an operating charge for the summer as well as the charge required to flood the condenser

for winter operation. On the air side the calculator is able to determine the air leaving temperature and air pressure drop after passing through the condenser. Then to tie everything together, I did some system simulations and was able to estimate the system power consumption, system energy efficiency rating, and the estimated annual operating cost of the chiller.

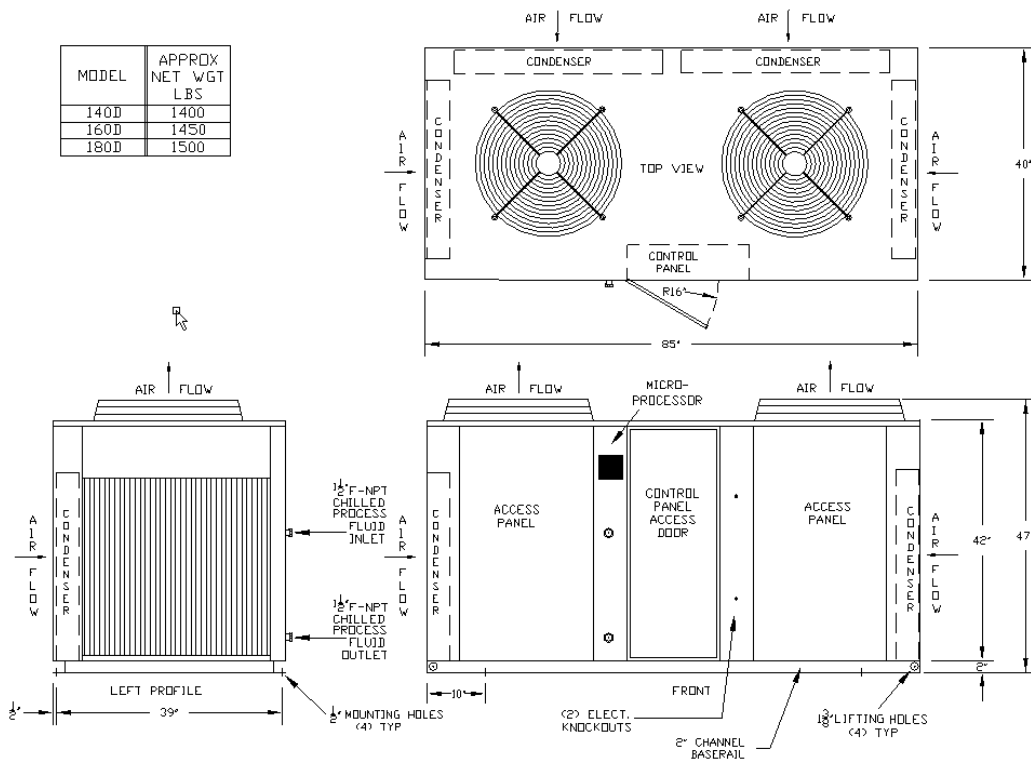
Report Objectives

The objective of this project is to study the design and optimization of an air-cooled condenser coil with a primary focus on altering the geometric design of the coil in a vapor compression cycle with R407c as the working fluid. The main goal of this project will be to design a minimum size condenser coil to allow for a compact chiller with cost being the second priority. There will be some set constraints due to material and product availability that will be taken into consideration. The simulation tool was initially designed for the chiller with a capacity of 150,000 btu/h (12.5 tons) that requires 200,000 btu/h (16.67 tons) of heat to be rejected. This would be designed at the industry standard of a 20-25F-temperature difference between the highest yearly ambient temperature in the area and the condensing temperature. This chiller would operate at a saturated suction temperature of 35F and have a superheat of 10F and a subcooling of 5-10F. This calculator would allow to specifically select the condenser geometric design parameters including the user overall condenser length and height, number of rows, number of circuits, row and tube spacing, fin thickness, fin density, tube inner and outer diameters, and the quantity and power of the fan motors. With all these user adjustable inputs for the calculator, it gives the user great flexibility and instant analysis of the condenser designed. Therefore a basic understanding of the refrigeration cycle is required to design and optimize the system.

APPROX NET WT 3600 LBS
 ALL ACCESS PANELS ARE HINGED & REMOVABLE



Dimensional drawing of PAC180S (With large and expensive horizontal condenser)



Dimensional drawing of PAC180D (With smaller vertical condensers)

Figure 1: Size Comparison of Existing Chillers (Drake Refrigeration 2016)

Chapter 2 - Background Chillers

Today chillers are often used in industrial applications where chilled water is pumped through processes or laboratory equipment. Industrial chillers are used for the controlled cooling of products, mechanisms and factory machinery in a wide range of industries. These process chillers are often used in the plastic industries, metal working cutting oil, welding, machine tooling, chemical processing, food and beverage processing, power supplies, compressed air and gas cooling, and medical equipment. Industrial chillers are also used to cool high heat items such as MRI machines and lasers. Chillers are used in hospitals, hotels, and college campuses when it is easier to pump water than to move air throughout an entire building. Chillers can be centralized for multiple industrial applications by using a single chiller that provides cooling for multiple loads.

A chiller is a machine that removes heat from a fluid by using the vapor compression cycle where the cooled fluid is then pumped for the controlled cooling of equipment or other processes. A necessary byproduct of the refrigeration cycle is the waste heat generated and this must be exhausted to the outside air. In air conditioning systems for multi-family homes, water is distributed to each home's localized heat exchangers in air handling units (AHU), which cools the air in their respective space. The water is then warmed by the exchange of heat in each AHU and then re-circulated back to the chiller to be cooled again. The AHU transfers the sensible and latent heat from the local air to the chilled water. These air-handling units are thus able to cool and dehumidify the local air. Typical chillers for air conditioning applications are rated between 1 ton and 2000 tons. The chilled water temperature delivered to the air handling units range from 35 to 45F depending on process requirements.

Chillers have other applications in addition to being used simply for air conditioning applications. Any piece of equipment or application that requires a chilled fluid for operation has the possibility of using a chiller to meet the demands. In the food processing market, chillers are used for breweries, wineries, dairies, food washing, water fountains and even bakeries. In the industrial market, chillers can be used to cool lasers, punch presses, injection molders, rocket fuel cooling, and welding machines. In the medical field, chillers can be used for MRI magnet cooling, CAT scan cooling, and in pharmaceutical labs. With all these process applications in varied markets it shows that a plethora of chillers have applications in more than just air

conditioning. Process chiller application sales make up 85% of the core business at Drake Refrigeration as compared to the 15% of sales where chillers are sold for air conditioning.

Chapter 3 - Background Refrigeration Cycle

Chillers studied in the project use the vapor compression cycle, with R-407c refrigerant as the working fluid. Shown below in Figure 2: “Temperature vs. Entropy Diagram” is the refrigeration cycle that a chiller undergoes to exchange heat with water. In Figure 2, at State 1 the diagram shows low pressure, superheated refrigerant vapor exiting the evaporator and entering the compressor that then leaves the compressor as a high pressure, superheated vapor in State 2. This hot vapor enters the condenser at State 2 and from State 2 -3 this is where the waste heat must be rejected to the outside air by moving outside air through the condenser coil. From the compressor at State 2 the refrigerant vapor is cooled by the condenser to the saturation temperature in State 3’, and then continues cooling until all the vapor becomes a liquid in State 3. In this plot the refrigerant is cooled along the saturation line achieving state 4. In actual cases the refrigerant is cooled below the saturation point for 5-10 F until only subcooled liquid would be present in this state. The high-pressure liquid in State 4 is then forced through a restriction, the expansion valve, to lower the pressure and temperature of the refrigerant to a temperature less than the load in State 5. The refrigerant enters the evaporator and absorbs heat from the warm fluid that is moved through the evaporator. Upon exiting the evaporator, the liquid-vapor refrigerant mixture enters the evaporator, absorbs heat while converting to a saturated vapor at State 6. The refrigerant is then heated beyond that temperature, where superheating occurs before entering the compressor in State 1. The water is cooled as it flows through the evaporator and returned to the process at a lower temperature.

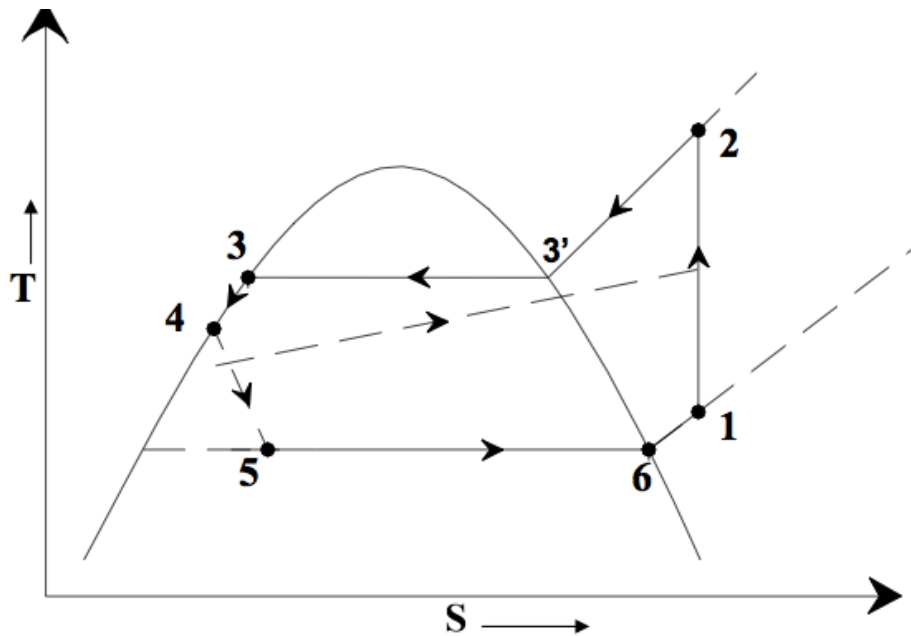


Figure 2: Temperature vs. Entropy Diagram (D.G. Rich 2009)

In this project the main focus will be on the design and optimization of the air cooled condenser coil. The condenser is a heat exchanger that removes heat from the refrigerant cycle to the outside air, which involves process 2 to 3 on the T-S diagram. In this project, the waste heat will be removed by pulling air over finned-tube condenser coils. Refrigerant flows through the tube, and a fan and motor forces air between the fins and over the tubes. The heat exchangers used in this project are cross-flow, plate fin and tube type. Shown below in Figure 3: “Cross-flow Heat Exchanger” is a display of air flowing across and over the horizontal tubes with flowing refrigerant inside the tubes. The plate fins are made out of aluminum and are not shown in this schematic to simplify the display. The plate fins are typically ordered in a fin per inch pattern ranging from 6 to 14 depending on the application. For environments where air blows a lot of debris or dirt around, i.e. a desert, then one would want fewer fins per inch to allow the debris to pass through. Air enters the condenser coil at the ambient air temperature from the left and is pulled through while extracting heat from the tubes and plate fins. The air absorbs heat as it is being pulled through the coil and then rejects it to the outside air until the coil temperature is greater than the outside air temperature. This exchange of heat to the ambient air is what will remove the waste heat from the refrigerant cycle.

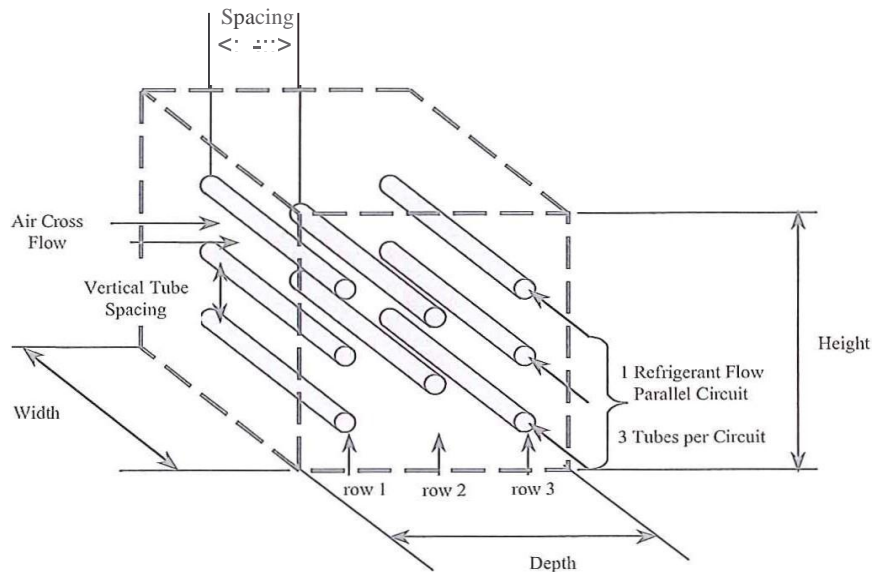


Figure 3: Cross-flow Heat Exchanger (Bergman 479)

When refrigerant leaves the compressor it enters the condenser as a superheated vapor and leaves as a couple degree sub-cooled liquid. The refrigerant enters the condenser to cool down and condense incoming refrigerant vapor in to liquid refrigerant. This is done in three sections of the condenser: superheated, saturated, and sub-cooled as shown in Figure 4: “Actual Vapor Compression Refrigeration Cycle”.

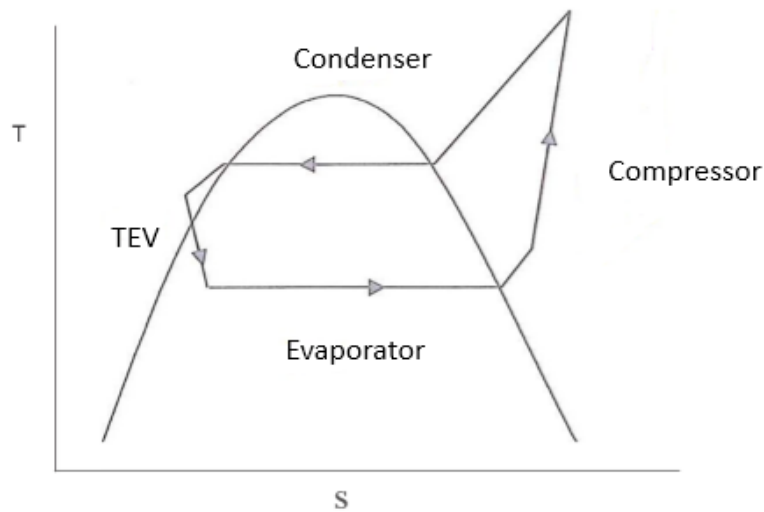


Figure 4: Actual Vapor Compression Refrigeration cycle (Jacobi 2006)

Inside the condenser the refrigerant will go through multiple tube passes that are surrounded by plate fins while the air moves through the condenser coil ultimately discharged by the fan. The motorized fan and blade assembly are mounted inside the top of the metal housing that pulls the outside air through the condenser coil.

Chapter 4 - Chiller System and Component Modeling

In the condenser coil, heat is exchanged between the refrigerant flowing through the tubes and the air being drawn through the coil. The ambient air passing through the coil extracts heat from the refrigerant transferring it to the air. This heat exchange between refrigerant and air must satisfy an energy balance since energy that is put into a system must be removed in order to return the system to equilibrium. Shown below in equation (1) is the total heat rejected on the airside, \dot{Q}_a . Where \dot{m}_a represents the air mass flow rate over the coil, $c_{p,a}$ is the specific heat of air, T_o is the air outlet temperature and T_i is the air inlet temperature. In equation (2) this is the total heat rejected from the refrigerant side, \dot{Q}_r . Where \dot{m}_r represents the refrigerant mass flow rate through all the condenser tubes, h_i is the enthalpy value of the superheated refrigerant entering the condenser, and h_o is the enthalpy value of the subcooled refrigerant leaving the condenser. Equations (1) and (2) are set equal in an energy balance.

$$\dot{Q}_a = \dot{m}_a c_{p,a} (T_o - T_i) \quad (1)$$

$$\dot{Q}_r = \dot{m}_r (h_i - h_o) \quad (2)$$

The total heat rejected from the refrigerant to the air is dependent on the heat exchanger effectiveness and the maximum total heat that can be exchanged is shown in equation (3), where E represents the heat exchanger effectiveness and Q_{\max} is the maximum total heat that could be exchanged.

$$\dot{Q} = E Q_{\max} \quad (3)$$

The maximum heat transfer occurs when taking the temperature difference between the temperature of air in, $T_{a,i}$, subtracted from the temperature of the refrigerant entering the condenser, $T_{r,i}$. This temperature difference is multiplied by C_{\min} , which represents the smaller heat capacities of the hot and cold fluid. The heat capacity of each fluid is calculated by multiplying the mass flow rate by the specific heat at conditions. This value of C_{\min} , is shown in equation (4).

$$C_{\min} = c_p \dot{m} \quad (4)$$

After calculating the value of C_{\min} in each section of the condenser the total heat transfer possible, Q_{\max} , can then be calculated as shown in equation (5).

$$Q_{\max} = C_{\min}(T_{a,i} - T_{r,i}) \quad (5)$$

Now that Q_{\max} is identified, the next step is the effectiveness, E , of the heat exchanger from equation (3). The condenser can be separated into three sections where heat is exchanged: superheated, saturated, and sub-cooled. The effectiveness of the heat exchanger needs to be separately calculated for each section and then combined. There are separate effectiveness equations for the single-phase superheated, and sub-cooled regions in conjunction with the two phase saturated region. These effectiveness equations are shown in equations (6) and (7). The saturated region is where the majority of the heat transfer occurs. In the saturated portion of the condenser the refrigerant heat capacity approaches infinity causing the ratio to go to zero. When the ratio goes to zero the saturated region equation reduces to equation (6).

2-Phase Region

$$E = 1.0 - e^{-NTU} \quad (6)$$

1-Phase Region

$$E = 1.0 - e^{-(1 - e^{(C_{\text{ratio}} * NTU)})/C_{\text{ratio}}} \quad (7)$$

“The heat exchanger effectiveness is dependent on the temperature distribution for each fluid and the path of the fluids” [2001, December 1, AKAspelund]. In this application the mass flow rates of refrigerant and air do not mix. Air temperature entering the condenser coil will not be the same as the temperature of the air exiting. The two-phase region effectiveness is less complicated due to the C_{ratio} going to zero in this region and therefore the equation is reduced to equation (6). The C_{ratio} equation as shown in equation (8) represents the comparison of the specific heats of each fluid.

$$C_{ratio} = \frac{c_{min}}{c_{max}} \quad (8)$$

For a cross-flow heat exchanger with both fluids unmixed, the effectiveness can be related to the number of transfer units (NTU) with a value calculated in equation (9).

$$NTU = \frac{UA}{c_{min}} \quad (9)$$

The number of transfer units is the function of the overall heat transfer coefficient, U, and A, which represents the heat transfer area. The overall heat transfer coefficient is made up from the thermal resistance between the two fluids exchanging heat. Equation (10) represents the total thermal resistance that is occurring between the refrigerant and air.

$$\frac{1}{UA} = \frac{1}{\eta_{sa}h_aA_a} + \frac{R_{fa}}{\eta_{sa}A_a} + R_w + \frac{R_{fr}}{\eta_{sr}A_r} + \frac{1}{\eta_{sr}h_rA_r} \quad (10)$$

The subscript “a” represents air and “r” represents refrigerant. A is the outside area for the air or refrigerant that heat is exchanged through. R_f is the fouling factor, R_w is the wall thermal resistance, $\eta_{s(a \text{ or } r)}$, is the surface efficiency and h is the average heat transfer coefficient. Equation (10) reduces since there are no fins on the refrigerant side of the condensing tubes, making the refrigerant side efficiency 1. The wall thermal resistance, R_w , is also neglected as it much smaller on an order of 0.01% than the other resistances. The fouling factors for air and water also have small magnitude and are also neglected. This reduces the overall heat transfer equation to:

$$\frac{1}{UA} = \frac{1}{\eta_{sa}h_aA_a} + \frac{1}{h_rA_r} \quad (11)$$

The overall surface efficiency is calculated by comparing the area of the fins, A_f , to the overall area, A_o . This is then multiplied by the fin efficiency, η_f , to yield the surface efficiency.

$$\eta_s = 1 - (1 - \eta_f) \frac{A_f}{A_o} \quad (12)$$

To determine the overall surface efficiency $\eta_{s(a)}$ for the finned heat exchanger it is necessary to find the efficiency of the fins, η_f , as if they existed alone. The first step is defining the transverse distance between copper tubes that is perpendicular to air flow, P_t , and longitude distance that runs parallel to air flow, P_l . For a fin and tube heat exchanger with multiple staggered tubes, the plates can be evenly divided into hexagonal shaped fins. The fins used on this condenser will have uniform cross sectional area in the shape of a rectangular. The fin length will be much greater than the fin thickness and therefore the magnitude of the ends will have minimal effect justifying the neglect of the ends in calculations. The fin density is designated by how many fins there are per inch and this typically starts around 6 fins per inch up to as high as 18 fins per inch.

The initial spacing variables that make up the spacing of the condenser tubes are XM and XL as shown in equations (13) and (14). XM represents the transverse spacing for the air flow perpendicular to flow. XL represents the diagonal spacing between the staggered tube patterns.

$$XM = \frac{P_t}{2} \quad (13)$$

$$XL = 0.5 \left(\frac{P_t^2}{2} + P_L^2 \right)^{0.5} \quad (14)$$

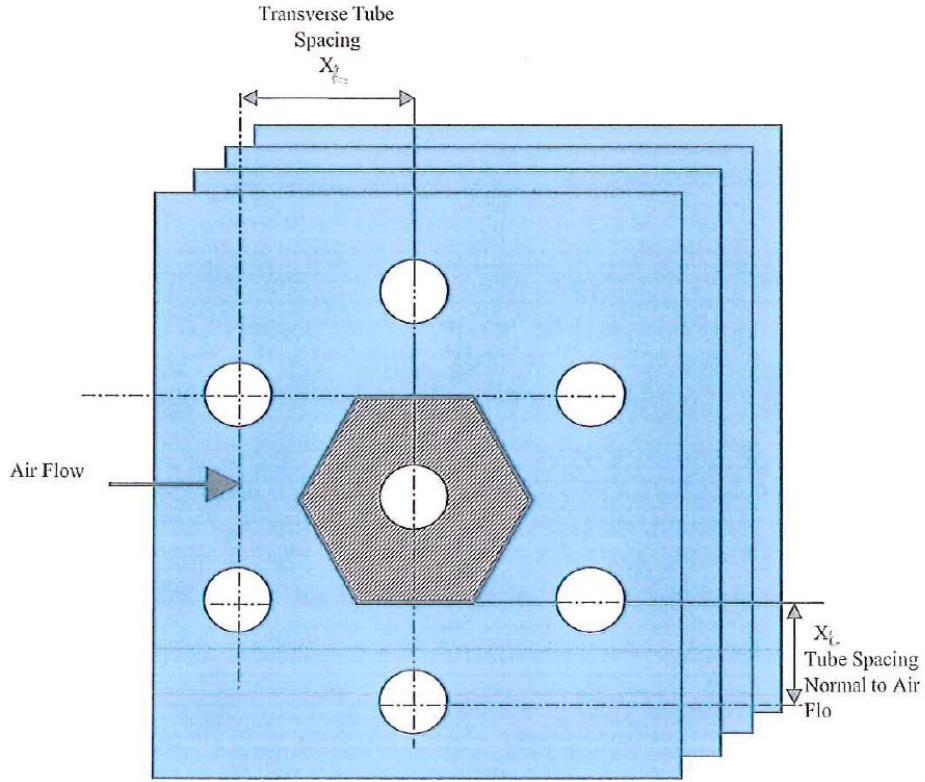


Figure 5: Staggered Tube Arrangement in Bank of Condenser (AKAspelund 5)

AKAspelund (1) analyzed hexagonal fins as shown in Figure 5 and determined that the equations for standard circular fins could be used to replicate this fin pattern. The equivalent radius can be calculated using equation (15).

$$r_{eq} = 1.27XM \left(\frac{XL}{XM} - 0.3 \right)^{0.5} \quad (15)$$

The equivalent radius, r_{eq} , will allow the fin pattern to be represented using the circular fin pattern. For circular tubes the next parameter that needs to be defined is the ϕ and is shown in equation (16).

$$\phi = \left(\frac{r_{eq}}{r_{collar}} - 1 \right) \left(1 + 0.35 \ln \frac{r_{eq}}{r_{collar}} \right) \quad (16)$$

Where r_{collar} is the outer diameter of the copper tube plus two times the fin thickness. The next parameter for circular fins is the LL, which is represented by equation (17).

$$LL = \phi * r_{collar} \quad (17)$$

Once the equivalent radius has been determined, the extended surface parameter, mm, is expressed as:

$$mm = \sqrt{\frac{2h_o}{t_f k_f}} \quad (18)$$

where h_o is the air side heat transfer coefficient, k is the fin thermal conductivity, and t is the fin thickness. The fin efficiency, for the circular fin can then be expressed as a function of equation (18).

$$\eta_f = \frac{\tanh(mm*LL)}{mm*LL} \quad (19)$$

Equation (19) represents only the fin effectiveness for the condenser coil. This fin efficiency can now be put back into equation (12) to complete solving for the overall surface efficiency of the condenser coil.

4-2 Refrigerant Pressure Drop

In addition to finding the efficiency and capacity of the condenser, it is important to find the refrigerant pressure drop through the condenser. This is the pressure loss caused by the flow of refrigerant through the condenser tubes. This pressure drop is caused by the amount of refrigerant flowing through the tubes, the friction factor from the tube walls, and the path the refrigerant must take. The pressure drop of refrigerant through the entire condenser assembly is typically between 2-10 psi, based on my experience with other similar assemblies (Drake 2016). A large pressure drop in the condenser wants to be avoided in design, as it will result in a

decrease of efficiency of the chiller. This pressure drop calculation accounts for the entire path that the refrigerant will travel including, the straight paths and curved bends at the ends of the condenser. The refrigerant will undergo two-phase changes inside the condenser that will add to the pressure drop, from a superheated vapor to saturated mixture and from a saturated mixture to a subcooled liquid. Therefore, the calculation of a pressure drop through a condenser became a very complex formula and I was not able to produce a result that was within an acceptable range of 2-10 psi. Based on my experience, my initial calculations yielded pressure drops that were far too large for a condenser of this size (Drake 2016). Therefore, to simplify the pressure drop calculation, I decided to eliminate phase changes that took place inside the condenser for this calculation. This was done by eliminating the saturated refrigerant mixture region and only focusing on the superheated vapor and subcooled liquid traveling through the condenser. This simplification was done to help achieve results that were within an acceptable range of 10 psi or less. It was assumed that while the refrigerant is a saturated mixture that no pressure drop through this portion of the condenser took place. This is known to be inaccurate, but was balanced out by the calculated pressure drops in the superheated and subcooled condenser sections. The inaccuracies from the other regions do not justify the elimination of the pressure drop in the saturated region.

Another simplification that was rendered for accuracy was to eliminate the bends at the end of the condenser from the refrigerant path leaving only the straight lengths of the condenser path. The overall straight length of tubes inside the condenser was then used to calculate the overall pressure drop. It was assumed that the bends at the end of the condenser would have a minimal effect on the pressure drop and were therefore neglected. This was also found to be inaccurate, as much of the refrigerant pressure drop would occur in these bends due to the increased velocities at the end of the condenser.

After reviewing these assumptions, it was found that they did not merit any technical correctness. Due to their technical inaccuracy I would advise not making the same assumptions and calculating the refrigerant pressure drop differently.

However, with these assumptions the resulting pressure drops were found to yield results with an acceptable range based on my experience with testing similar size condensers (Drake 2016).

Therefore, based on these assumptions the pressure drop in straight tube portions of the superheated and subcooled sections can be determined by applying the pressure drop relationship shown in equation (20)

$$\Delta P = dP/dL_r(L_t) \quad (20)$$

where ΔP is the pressure drop, dP/dL_r is the pressure gradient, and L_t is the length of tube the refrigerant must travel through. The friction factor, f_{vap} , the total mass flux G_r , density, ρ_{vap} , and condenser tube inside diameter, d_i make up this portion of the equation for both the superheated vapor and subcooled regions. This is shown for the pressure gradient calculations in equations (21) and (22).

$$dp/dL_r = \frac{2f_{vap}G_r^2}{\rho_{vap}d_i}, \text{ Superheated} \quad (21)$$

$$dp/dL_r = \frac{2f_{liq}G_r^2}{\rho_{liq}d_i}, \text{ Subcooled} \quad (22)$$

The next step is to calculate the mass flux of refrigerant flowing through the tubes, G_r . The mass flux accounts for the amount of refrigerant that the compressor can push through the condenser by dividing the mass flow rate, m_{dotr} , and the cross sectional area of the condenser tubes. This mass flux equation is show in equation (23).

$$G_r = \frac{m_{dotr}}{A_{cs,t}} \quad (23)$$

The friction factor will need to be calculated separately for each section of the condenser to get a total pressure drop. The different sections of the condenser will result in different velocities through the tubes. In the vapor regions the friction factor is calculated by using the following

equation for turbulent flow:

$$f_{vap} = \frac{0.046}{Re^{0.2}}, \text{ Turbulent flow} \quad (24)$$

where Re represents the Reynolds number for the refrigerant traveling through the tubes. For the refrigerant, the Reynolds numbers can vary from 21,000 to 1,500,000. The friction factor for refrigerant with a Reynolds number below 2,300 is calculated as shown in equation (25) for laminar flow.

$$f_{liq} = \frac{0.079}{Re^{0.25}}, \text{ Laminar flow} \quad (25)$$

The Reynolds number for each portion is calculated using the standard equation below in equation (26). The ρ , represents density, V represents velocity of the refrigerant, D represents the diameter, and μ represents the dynamic viscosity of the fluid. In order for a fluid to be flowing in the turbulent region it must have a Reynolds number above 2100.

$$Re = \frac{\rho V D}{\mu} \quad (26)$$

These equations can then be used to work backwards to find the pressure drop through each portion of the condenser.

4-3 Air Pressure drop

Heat transfer from a bank of tubes in cross-flow is relevant in many applications including air conditioning and even chillers. Air moves over and around the tubes starting at ambient temperature while the second fluid, refrigerant passes through the tubes at a higher temperature. The rejection of excess heat from the refrigerant cycle takes place in the air-cooled condenser. The tubes can either be aligned or staggered in the direction of the airflow velocity, however most manufacturers for refrigeration use staggered tubes. The tube diameter, transverse pitch, St, longitudinal pitch, Sl, and fins per inch need to be specified by the designer for the design of the condenser.

First to be calculated is the maximum velocity of air that can travel through the condenser coil using equation (27). This can occur at the transverse plane, A1, or the diagonal plane, A2 as shown in Figure 6: “Staggered Tube Layout Side View.”

$$V_{max} = \frac{S_t}{S_t - D} V \quad (27)$$

Where V represents the nominal velocity of the air that a condenser fan can pull across the coil, D is the coil diameter and S_t , is the transverse pitch between tubes. In this staggered coil application, the maximum velocity occurs at A1 as shown in Figure 6.

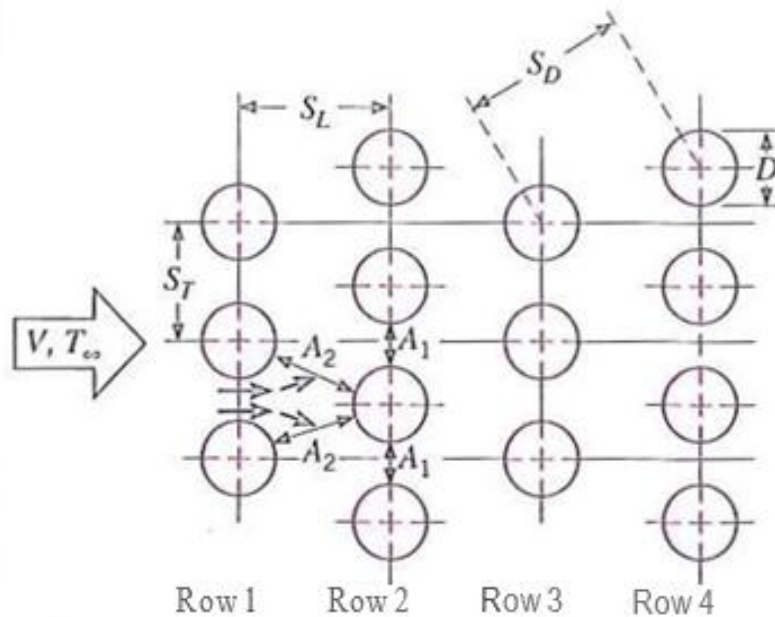


Figure 6: Staggered Tube Layout-Side View (Bergman 469)

Once the maximum air velocity is calculated, this result will be used to find the maximum Reynolds number of air moving through the coil as shown in equation (28), where ν represents the kinematic viscosity of the air at the conditions of the unit. Thus,

$$Re_{D,max} = \frac{V_{max}D}{\nu} \quad (28)$$

The maximum Reynolds number can then be used to calculate the average Nusselt number. The Nusselt Number, Nu is the ratio of the convective to conductive heat transfer across the boundary. The equation for the average Nusselt number to represent the entire tube bank is shown below in equation (29).

$$Nu_D = C_1 C_2 Re_{D,max}^m Pr^{0.36} \left(\frac{Pr}{Pr_s}\right)^{0.25} \quad (29)$$

where C1 represents the constants of equation for a tube bank in cross-flow for staggered configuration with St/SL less than 2, with a Reynolds max number between 10³ to 200,000 (Bergman 471). From this same table, the m factor is defined with a value of 0.60.

$$C_1 = 0.35 \left(\frac{St}{S_L}\right)^{1/5} \quad (30)$$

The variable C2 represents the correction factor for a bank of tubes with less than 20 rows and a Reynold's max number greater than 1000 as shown in Table 1: "Correction Factor Table" below.

Table 1: C2 Correction Factor Table (Bergman 2011)

# Rows	1	2	3	4	5	7	10	13	16
Correction Factor	0.64	0.76	0.84	0.89	0.92	0.95	0.97	0.98	0.99

The Prandtl number, Pr, of the fluid is a dimensionless number defined as the ratio of momentum diffusivity to thermal diffusivity. The Prandtl number for air was simply taken from a built in air properties table for the ambient air temperature for the excel program. The surface Prandtl number, Pr_s, is generated within the "calculator" based on the condenser tube surface temperature. These values will then allow one to calculate the average Nusselt number, Nu, for a fluid.

The next important piece of information that can be gathered is the maximum pressure drop that occurs to the air as it passes through a bank of tubes. This pressure drop is found using equation (31) below (Bergman 2011). To find the nominal pressure drop through the tubes, the V_{max} is adjusted by using the operating air velocity as compared to the maximum air velocity,

$$\Delta p_{max} = N_L X \left(\frac{\rho V_{max}^2}{2} \right) f \quad (31)$$

where N_L represents the number of rows, X is a correction factor that is plotted in Figure 7, f represents the friction factor, ρ represents the density, and V_{max} is the maximum velocity of air flowing through the bank of tubes.

The friction factor and X value can both be gathered from Figure 7: “Friction Factor and Correction Factor for Staggered Tube Arrangement (Bergman 2011)”.

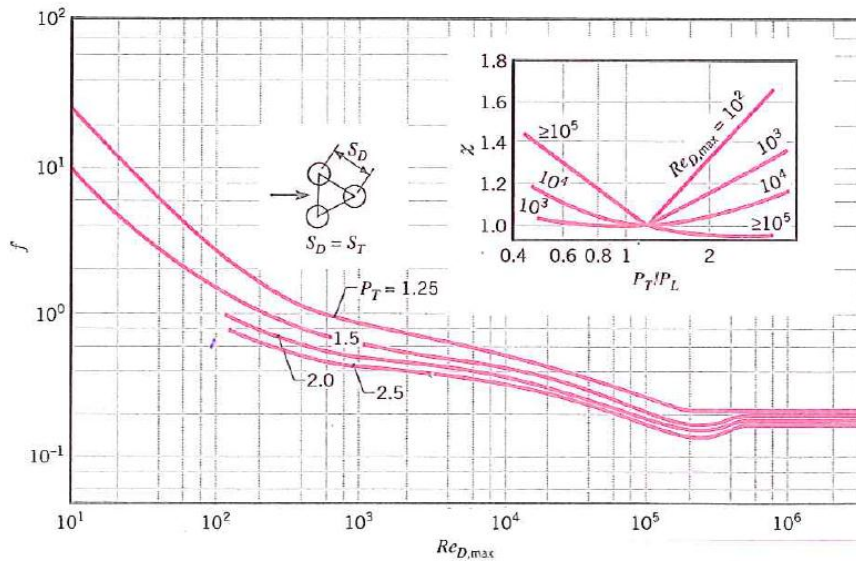


Figure 7: Friction Factor and Correction Factor for Staggered Tube Arrangement (Bergman 2011)

Finally, this can all be put together to calculate the maximum and nominal pressure drop across a bundle of tubes. The fan blade industry uses a unit of inches in water column as compared to the

standard psi. This conversion is done from psi to inches of water column by multiplying the psi by 2.707 inches H₂O.

4.4 Air leaving temperature

As the air passes through the bank of tubes comprising the condenser, the air temperature will rise from the initial ambient temperature towards the surface temperature of the tubes. This difference in temperature causes heat transfer to occur between the air and refrigerant as it moves through the condenser coil. An important aspect of condenser sizing is to ensure that the air leaving temperature does not become too high causing damage to the fan motor or refrigerant circuit itself. The outlet air temperature may be calculated by using the following equation.

$$T_o = T_s - [(T_s - T_i)\exp(-\frac{\pi DNh}{\rho V N_T S_T c_p})] \quad (32)$$

In equation (32), the temperature T_o represents the outlet temperature of the air, T_s represents the surface temperature of the tube, and T_i represents the inlet temperature of the air. On the right side of the equation D is the condenser tube diameter, N is the total number of tubes in the condenser, N_t is the number of tubes per row, h is the average enthalpy between the air temperature and tube surface temperature, V is the air velocity, ρ is the air density, S_t is the distance between tubes, and c_p is the specific heat of air at the average temperature.

4.5 System Performance

In order to evaluate the overall performance of a condenser coil, the overall system must be analyzed to be able to compare to other systems. For a chiller utilizing a vapor compression cycle, the efficiency is expressed in terms of the cooling or coefficient of performance (COP). The COP is a ratio of the refrigeration capacity compared to the electrical and mechanical power

used by the chiller to drive the system. The coefficient of performance is a dimensionless quantity. In chillers this power comprises the compressor power, condenser fan power and other small power consumers represented by W_{etc} . This is shown below in equation (33).

$$COP = \frac{Q}{W_{compr} + W_{cond} + W_{etc}} \quad (33)$$

The Q represents the refrigeration capacity of the system and the W represents the work from the different components required to make the system operate. In the United States, the performance of a chiller is often given in dimensional terms with the units of Btu/(W-hr), as an energy efficiency rating (EER). Since 3.412 Btu is equivalent to 1.0 W-hr, an EER rating of 10 would equal a COP of 2.93. In air conditioning it is more common to use the seasonal ratings including the $COP_{seasonal}$ or the SEER (season energy efficiency rating). The seasonal ratings takes into account the varying outside temperatures and the effect it has on the performance of the machine. However, with the process chiller market, the standard COP and EER are typically used due to processes requiring year round operation.

Chapter 5 - Optimization Parameters

When designing and optimizing a condenser coil to yield the maximum EER, there are many parameters that can be varied. In this study, these optimization parameters have been divided into categories, operating system parameters, and geometric design parameters. In order for an effective study to take place, comparisons between the systems EER can be made but must be between similar condenser coil configurations. It is not a fair playing field if one is to compare a 4 row condenser coil to a system with 2 rows. Therefore, in this project the performance of each configuration at the optimum operating conditions will be determined and compared.

5.1 Operating Parameters

The operating parameters of a system that are studied are the ambient dry bulb temperature, the amount of superheat exiting the evaporator, the amount of subcooling exiting the condenser, the amount of air moving through the condenser, and the velocity of the air flowing over the condenser. For this study, the amount of superheat exiting the evaporator is fixed at 10 F, which is required by many compressor manufacturers to prevent liquid from returning to the compressor. The ambient dry bulb temperature of 95 F will be used to run and rate the system, as this is the local design temperature in Philadelphia. The volumetric rate of airflow, the velocity of air moving over the condenser, and the subcooling are the three operating parameters that will be optimized for each condenser geometric configuration.

5.2 Geometric Parameters

There are a large number of condenser coil geometric design parameters that can be varied to optimize the performance of a chiller. These parameters include fin length, fin height, tube diameter, tube spacing, fin density, number of rows, and number of tubes per row. For this study the finned tube length, finned tube height, and number of rows will be optimized. In all cases the vertical and horizontal spacing is fixed at 1.000 in. and 0.866 in. respectively. These values are typical of the condenser coils that are manufactured for the industry and used by Drake. The condenser tubes will also be made using an industry standard rifled copper tube with an outer

diameter of 0.375 in. and wall thickness of 0.012 in. for product standardization. The condenser fins will have standard sine wave fins and will be aluminum. By using industry standard materials and spacing, the scope of this project will not creep beyond the main objective of optimizing the condenser for this system.

5.3 Optimization of the Operating Parameters

The performance of a chiller system is dependent on the specific operating conditions and parameters of the chiller. A nominal 10 ton chiller may do 10 tons at nominal conditions (35 F saturated suction temperature and 95 F ambient) but may only do 4 tons at a colder temperature of 10 F saturated suction temperature and 95 F ambient. Without defining the operating conditions, it is not possible to determine the condenser configuration that yields the highest EER. Again, the operating parameters investigated for this study are the volumetric airflow, air velocity, and amount of subcooling. To determine the effects of these parameters on the standard EER, a typical condenser is selected for the base line configuration. All the characteristics of the condenser are specified and the dimensions are shown in Table 2.

Table 2: Baseline Condenser Characteristics

Condenser parameters	Dimensions
Tube Spacing (in x in)	1.000 x 0.866
Tube inner diameter (in)	0.363
Tube outer diameter (in)	0.375
Height (in)	36
Fins per inch	12

Using this standardized condenser, Figure 8 shows the effects that the operating parameters have on the overall efficiency of the unit. The 70 in. x 36 in. condenser was selected as a baseline test. As the figure shows, there is a gradual improvement in the overall system efficiency of the unit as the airflow is increased. As the air flow rate increases for a fixed sized condenser, the air

velocity will also increase. Therefore, the volumetric air flow rate over the condenser is one of the operating parameters that will be optimized for each condenser configuration that is studied.

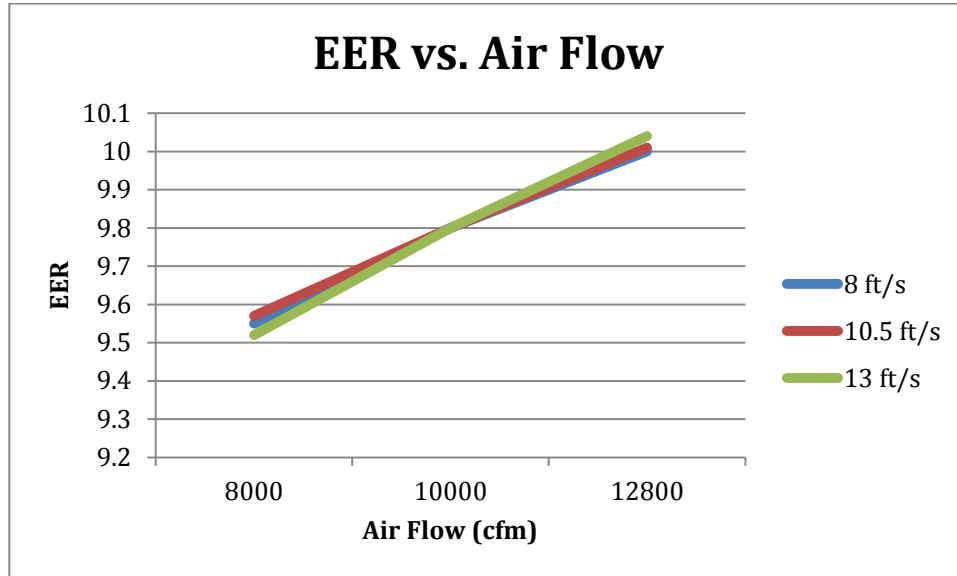


Figure 8: Effect of Operating Conditions on 70 in. x 36 in. Condenser

5.4 Effects of Volumetric air flow, Air velocity, and Subcooling

After developing a baseline test using the 70 in. x 36 in. condenser several different condenser frontal area sizes were then tested and compared. For this study the goal is to minimize the overall frontal area of the condenser while still allowing for an overall energy efficient unit. A standardized height of 36 in. was selected as being the tallest allowable condenser that can currently fit in the existing chiller assemblies. Therefore the length of the condenser coil and the number of rows were then adjusted to allow a wide range of condenser areas to be tested. The condensers that were evaluated are shown below in Table 3: “Simulated Condenser Sizes.” The range goes from shorter condenser lengths with more rows to longer condenser lengths with fewer rows. This range of condensers simulated would allow for a comparison of compact condenser sizes with multiple rows to wider condenser sizes with fewer rows. The condenser sizes were then compared for the resulting saturated condensing temperature, air leaving temperature, air pressure drop, and system EER.

Table 3: Simulated Condenser Sizes

Length (in.)	Height (in.)	Rows
40	36	8
50	36	7
60	36	6
70	36	5
80	36	4
90	36	3

5.5 Liquid Subcooling

Liquid subcooling is required to ensure that only liquid is entering the expansion valve with no bubbles present. Vapor bubbles present in a liquid line sight glass indicate a system that is low on refrigerant flow rate due to a low charge. Low refrigerant charge will cause a loss of capacity and efficiency in a chiller system. Chiller manufacturers require 5-10 F of liquid subcooling to ensure a proper charge and no loss of efficiency. Subcooling occurs when the liquid refrigerant exits at a temperature below its normal boiling point after moving through the condenser coil. When the refrigerant is below the saturation point it is now possible for the refrigerant to undergo the remaining stages of the refrigeration cycle more efficiently. Therefore, it is important to monitor and adjust the amount of subcooling that occurs in a refrigerant system. This is accomplished by comparing the liquid refrigerant temperature and the pressure after the condenser. The pressure is then converted to a temperature using a P-T chart and the two values are subtracted yielding the subcooling quantity. The amount of subcooling is directly related to the quantity of the charge in a system. By increasing the refrigerant charge, it is possible to increase the amount of subcooling that is occurring. However, one must not over charge a system with excess refrigerant, as the system would lose efficiency. The greater the amount of subcooling that a system has, the higher the saturated condensing temperature will be. This is the saturation temperature of the vapor refrigerant corresponding to the refrigerant pressure when entering the condenser. Therefore, the condensing temperature is directly affected by the amount of subcooling that was occurring. In this study, the amount of subcooling simulated for each condenser coil 0 F, 5 F, and 10 F. As shown below in Figure 9: “Saturated

Condensing Temperature vs. Subcooling,” there is an increase in condensing temperature as subcooling increases.

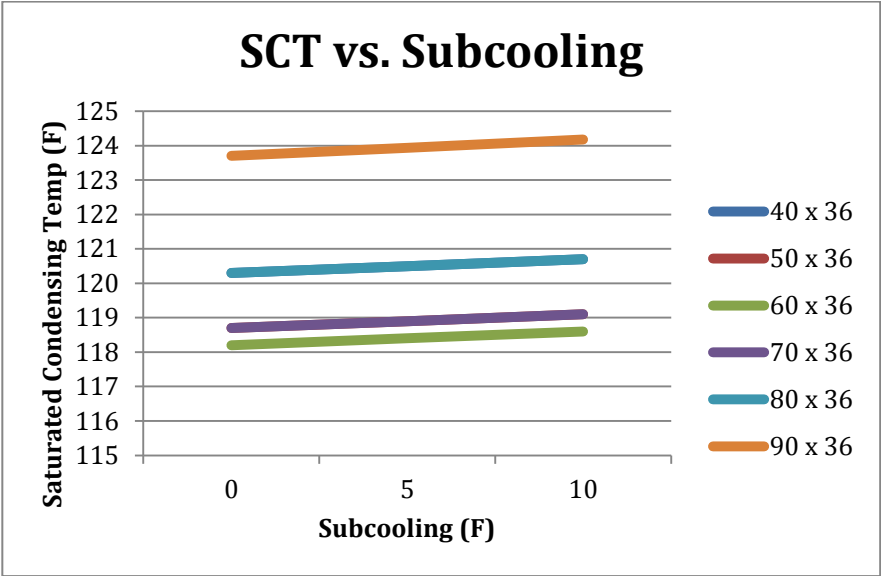


Figure 9: Saturated Condensing Temperature vs. Subcooling

As shown in Figure 9 for each condenser coil as the subcooling increases for each condenser, the saturated condensing temperature also increases. Directly correlated with the coil surface area is the initial condensing temperature. In Figure 9 the focus is on the slight increase of each coil’s saturated condensing temperature due to the increase in subcooling. Since the saturated condensing temperature is increased with the more subcooling that occurs in the system, the efficiency of the chiller is decreased.

In order to equally compare chillers to each other, an efficiency rating system was devised which is known as a system EER. EER stands for Energy Efficiency Rating and is calculated by comparing the chiller capacity output (in BTU) over the power consumed (in Watts) to generate this rating. Chiller manufacturers and consumers use EER to discuss products so as to have a level playing field. As shown in Figure 10: “EER vs. Subcooling”, as the subcooling is increased in a system the efficiency of the unit decreases. In each condenser coil that was simulated, there is a drop in the system EER due the increase in subcooling. The subcooling will cause the saturated condensing temperature to increase, which causes the compressor to run hotter, which in turn decreases chiller efficiency. So there is a delicate

balance between ensuring that the system is properly charged while not decreasing efficiency of the chiller.

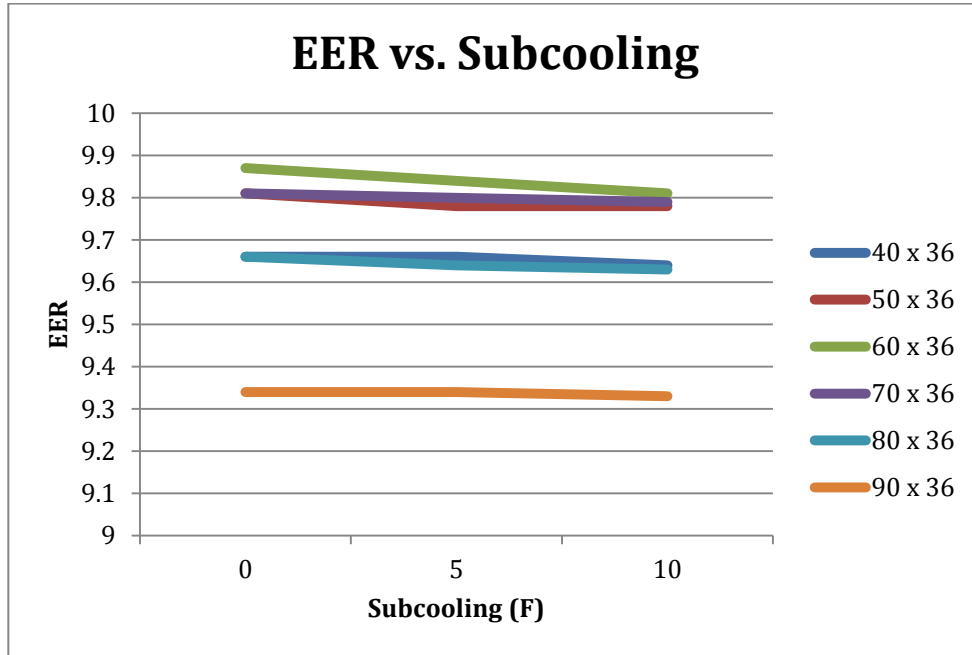


Figure 10: EER vs. Subcooling

5.6 Volumetric Airflow

Volumetric airflow is the amount of air that is pulled through a condenser coil within a unit of time often measured in cubic feet per min (cfm). During the refrigeration cycle, excess heat is generated when the refrigerant is compressed from a low-pressure superheated vapor to a high-pressure superheated vapor by the compressor. In order for the refrigeration cycle to operate, the excess heat must be removed from the cycle by the air-cooled condenser, fan motors, and fan blades. The condenser takes the high-pressure superheated vapor down to a high-pressure subcooled liquid. In air-cooled condensers this is done by pulling outside air across the condensers and discharging it to the environment. In the chiller assemblies investigated here, the condenser is mounted vertically and the fan motor and blades are mounted above the condenser horizontally as shown in Figure 11: “Common Chiller Assembly.” This setup allows the air to extract heat as it moves through the condenser coil and then discharge above the chiller. The reason it is discharged above the chiller is to ensure that hot air does not recirculate back through the condenser, and to counteract buoyancy.

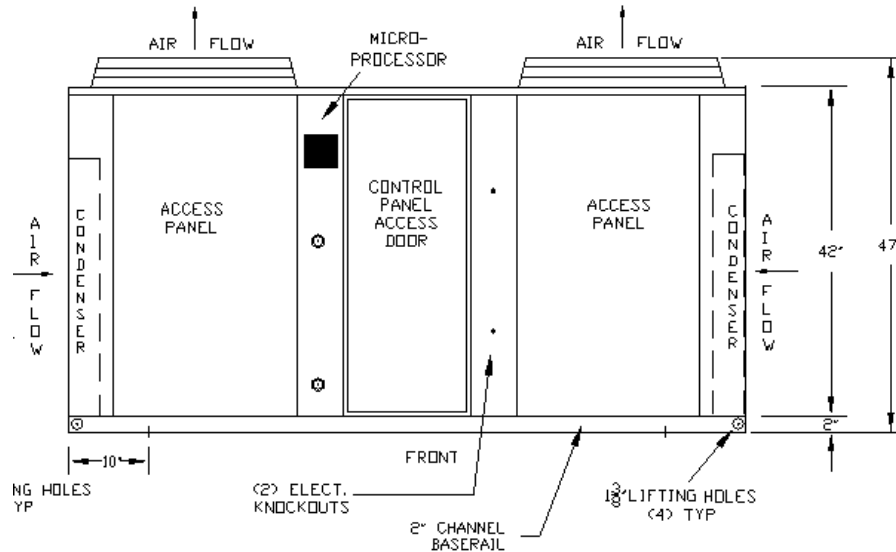


Figure 11: Common Chiller Assembly (Drake Refrigeration)

Therefore, the amount of air that is being pulled across the condenser will have a direct effect on the operation of the chiller. In the refrigeration cycle the compressor will operate and cause the condensing temperature to rise to a point where the temperature difference between the condensing temperature and the surrounding ambient is great enough to reject heat. This temperature difference is the driving force for heat transfer to take place. The greater the temperature difference the greater the heat transfer. More airflow will result in more heat transfer from the refrigerant to the surrounding ambient. In these simulations the ambient air is assumed to be 95 F and the compressor operated with a consistent capacity and amount of heat required to be rejected. Each condenser was then simulated with three different volumetric airflows: 8,000 cfm, 10,000 cfm, and 12,800 cfm. This is shown in Figure 12: “Saturated Condensing Temperature vs. Volumetric Airflow” where as the airflow increases, the saturated condensing temperatures decreases. The design for most condensers is to have a temperature difference between an ambient of 95 F and saturated condensing temperature of 20-30 F. This would result in a condensing temperature between 115 F-125 F. Therefore, it is desirable when designing a condenser to move enough air through the condenser in order to meet the desired temperature difference.

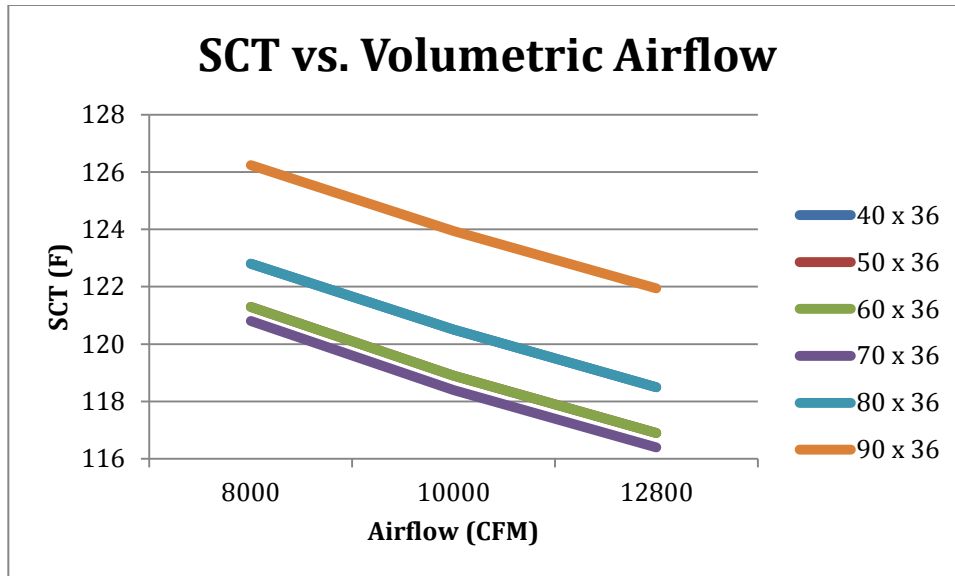


Figure 12: Saturated Condensing Temperature vs. Volumetric Airflow

Volumetric airflow has an inverse relationship with saturated condensing temperature. The higher the quantity of air that moves through the condenser the lower the system’s saturated condensing temperature. In this plot at 10,000 cfm, the condensers that are below 30F temperature difference include: 70 in. x 36 in. x 5 rows, 60 in. x 36 in. x 6 rows, 80 in. x 36 in. x 4 rows, and 90 in. x 36 in x 3 rows. This offers a wide range of condensers that are capable of maintaining the saturated condensing temperature at an appropriate level.

As shown above in the subcooling section, the greater the saturated condensing temperature the lower the EER. In regards to airflow, the greater the airflow the lower the saturated condensing temperature will be. The lower the SCT, the higher the efficiency of the system will be able to operate at. This is shown in Figure 13: “EER vs. Volumetric Airflow”. As the quantity of air pulled through the condensers is increased, the higher the system EER. There is a gradual increase in all of the condensers EER to between 9.5-10 rating.

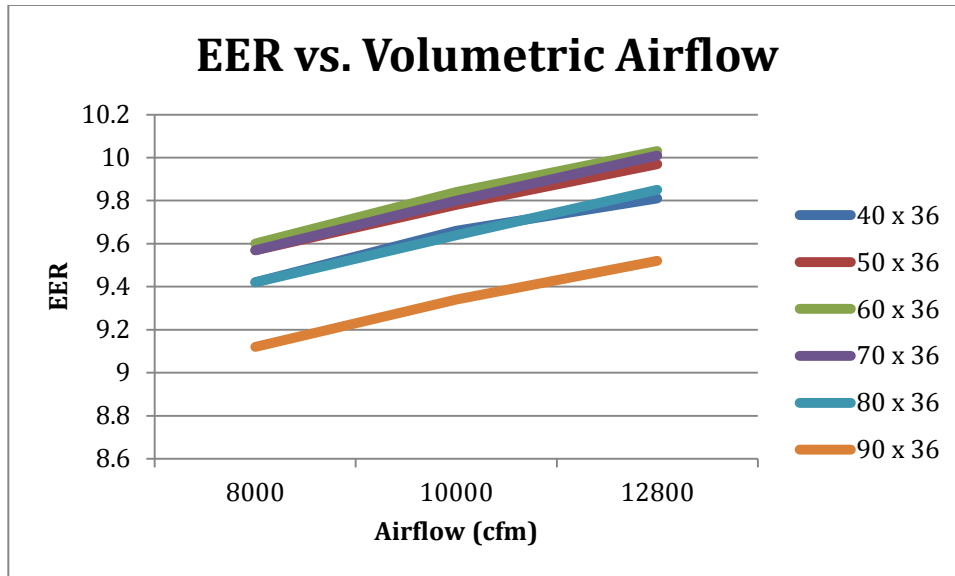


Figure 13: EER vs. Volumetric Airflow

However, there is a balance to selecting the proper airflow as there is a limitation based on the fan motor and blade that is selected. The fan blade and motor combination must be sized to overcome the pressure drop when moving this amount of air through the condenser coil.

5.7 Air Velocity

Heat transfer may occur from a bank of tubes in cross-flow and this method is used in many industrial applications including steam generation in a boiler and cooling the coil of an air conditioner, or in this case, a chiller. Air flows over the tubes while the refrigerant at a higher temperature passes through the tubes. The geometric arrangement of the bank of tubes will drastically affect the heat transfer rate. As discussed previously, the tube bundle can be arranged in an aligned or staggered pattern. The condenser coils were all simulated with a staggered tube pattern, as this has been standard on other pre-existing coils currently used at Drake. The tube spacing that was used in this study was 1.0 in. vertically x 0.866 in. horizontally between copper tubes. In addition to tube arrangement the largest contributing factor to air velocity is the fan motor and blade assembly. Two ¾ hp fan motors with 24-inch diameter fan blades were used to pull outside air through the condenser coils. When air is pulled through a bundle of tubes, the path with which the air must travel through creates a pressure drop. The staggered tube

arrangement forces the air to move through small spaces in between rows as shown in Figure 14: “Staggered Tube Arrangement in a Bank” (Bergman 2011).

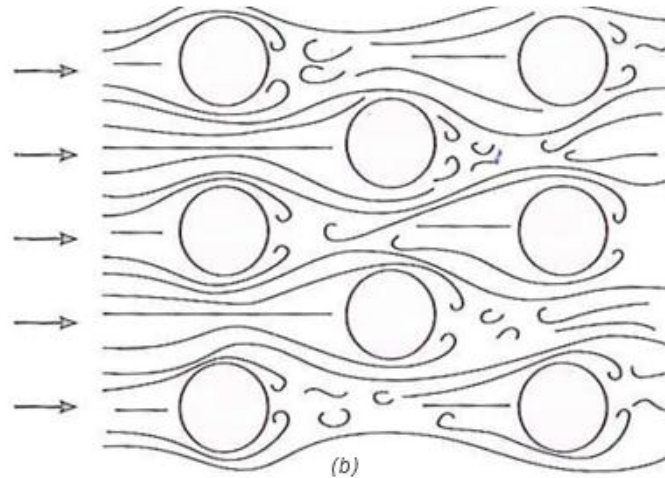


Figure 14: Staggered Tube Arrangement in a Bank (Bergman 2011)

The pressure drop must be overcome by the fan motor and blade in order for air to travel through the coil and remove excess heat from the refrigeration cycle. Pressure drop through a condenser coil is measured in inches of water gauge, which is the pressure required to support a column of water to a specified height. Shown below in Figure 15: “Air Pressure Drop vs. Air Velocity” are the results of the simulated condensers. As shown in the chart, as the air velocity increases, the greater the pressure drop through the condenser coil. Recalling Table 3: “Simulated Condenser Sizes”, see that condenser coils that have a shorter length have more rows. For example, the condenser coil that is 40 in. x 36 in. has 8 rows while the 90 in. x 36 in. has 3 rows. At the lower velocity of 8 ft/s, the pressure drop difference was minimal between the condenser coils. At higher air velocities, the pressure drop increased exponentially.

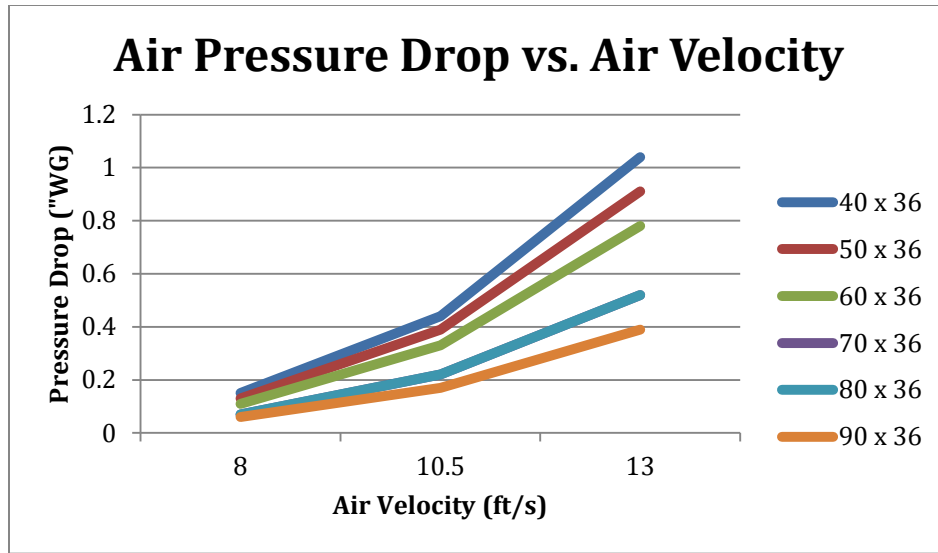


Figure 15: Air Pressure Drop vs. Air Velocity

There is a balance between the speed with which air is moved through a coil and maintaining a low air pressure drop. By keeping a low-pressure drop, one can use a less powerful fan to move the same amount of air. This smaller fan consuming less power would in turn increase the efficiency of the unit. This makes the air pressure drop an important factor when selecting a motor and blade assembly.

In addition to the air pressure drop, air velocity has a direct effect on the temperature of the air that flows through the condenser coil and exits to the environment. The heat transfer rate from the refrigerant to the air is greater when there is more time for the hotter fluid to come in contact with the cooler air. This is shown in Figure 16: “Air Leaving Temperature vs. Air Velocity”. For each condenser coil that was simulated, the air leaving temperature decreases with increasing air velocity. The condenser coils having more rows have higher air leaving temperatures resulting in more heat exchanged to the air. As a result, as the rows of the condenser coils decrease, so does the air leaving temperatures.

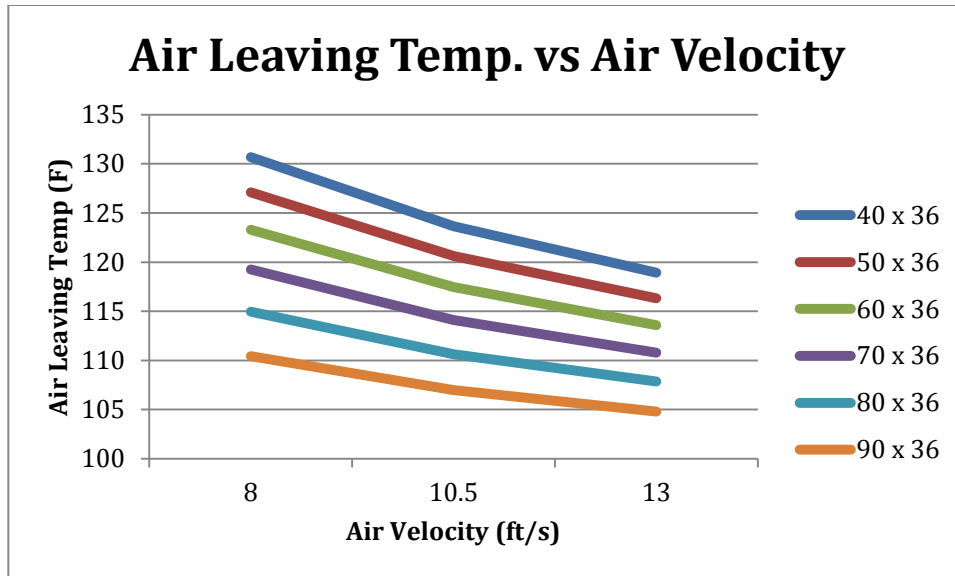


Figure 16: Air Leaving Temperature vs. Air Velocity

In order to standardize this study, two preexisting $\frac{3}{4}$ horsepower fan motors and fan blades with 24-inch diameters and 4 blades were used. When selecting a fan motor and blade assembly, careful consideration was given for optimization. Several different fan and motor combinations were evaluated to obtain the most efficient pairing.

5.8 Range of Optimum Operating Parameters

Based on the results discussed in this section, it is clear that there are ranges of operating parameters that yield a safe performance for the base system. Safe performance is based on the condenser assembly allowing the refrigerant to condense at an acceptable level to alleviate the system from reaching higher discharge pressures. By keeping the discharge pressures down, it makes for a safer system that operates at lower pressures to help the life of the system. It is determined that systems with 5 F of subcooling in the condenser yield safer and more efficient units per compressor manufacturers standards. Systems that have a total air flow moving through the condenser of 10,000 to 12,800 cfm will result in lower saturated condensing temperatures and will improve the efficiency of the system. Systems that have air velocities of 10.5 ft/s yield lower air pressure drops and more heat exchanged. These results will yield the optimum EER for the base configuration investigated in this study.

Chapter 6 - System Optimization

The two most pertinent constraints on the design of the condenser are the area requirements and overall cost. In this study the condenser frontal area is the most important geometric design variable and the one to be optimized. The frontal area of the condenser will affect the volume of the entire system. In order to optimize a condenser coil size for industrial applications, many constraints would need to be taken into consideration. The goal of this project is to design a condenser coil having minimum size that enables a compact 12.5-ton single circuit chiller to be manufactured effectively.

The first restriction that would need to be overcome is the physical size of the chiller. The preexisting dual circuit, 15-ton chiller has the following physical dimensions of 85 in. long x 45 in. high x 40 in. wide. This single circuit 12.5-ton chiller would need to be able to fit into this size cabinet in order to be an effective chiller in our product line. The dual circuit chiller, PAC180D, is shown below in Figure 17: “Overhead View of PAC180D” has condenser coils that are on two sides and the full backside of the unit. This was the existing condenser coil area that was required for the volume of airflow for this chiller to reject sufficient heat to the environment. Prior to building the “calculator” resulting from this study, condenser prototype experimental testing was required to optimize condenser size. Due to the large size of the required condenser coils, only the front side of the chiller is available for accessing the unit. Thus, repair or preventative maintenance is difficult because removing the electrical panel is needed to gain full access to the piping of the unit.

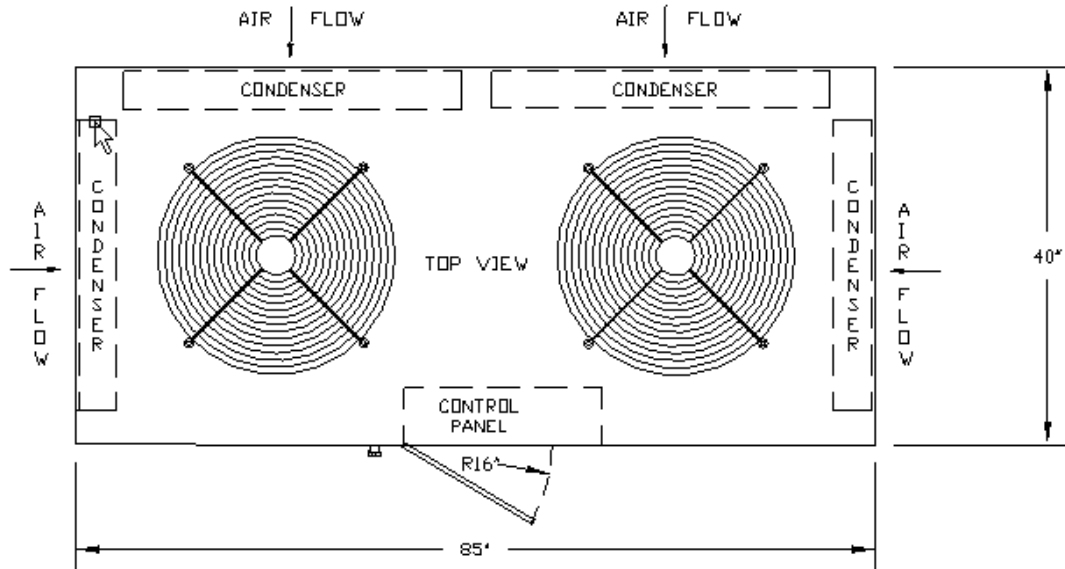


Figure 17: Overhead View of PAC180D (Drake Refrigeration)

To eliminate this issue, one of the goals of this study was to develop a smaller condenser area that would allow convenient access to the unit. Therefore, the goal was to develop a condenser coil frontal area that only required the backside length of the PAC180D unit. This reduced condenser area would enable a consistent chiller footprint along with maximizing access to the rest of the unit. Keeping the condenser coil length to less than 80 inches would allow ready access and easier maintenance for an ease of installation and operation.

The next restriction to overcome to making the optimized condenser fit the planned production line is using the current fan motor and blade assembly. This assembly is already predetermined across our product line based on manufacturing availability and the quantity discount we get by purchasing this many units. This assembly entails one or two (¾) horsepower fan motors with 24 in. diameter fan blades. Due to the required amount of airflow that is necessary to reject the excess heat, two fan assemblies are required for this simulated chiller. As shown in Figure 17 above, the two fan assemblies will be equally distant apart to evenly pull air across the coil. In addition to using the existing components, careful consideration must be taken into ensuring that the equipment will be able to function properly. The 24 in. diameter, four-blade propeller fan has a fan curve that shows pressure drop vs. volumetric airflow. This blades' fan curve is shown below in Figure 18: "Fan Curve" where the red line represents the static pressure drop in Inches-WG and the blue line represents the horsepower required.

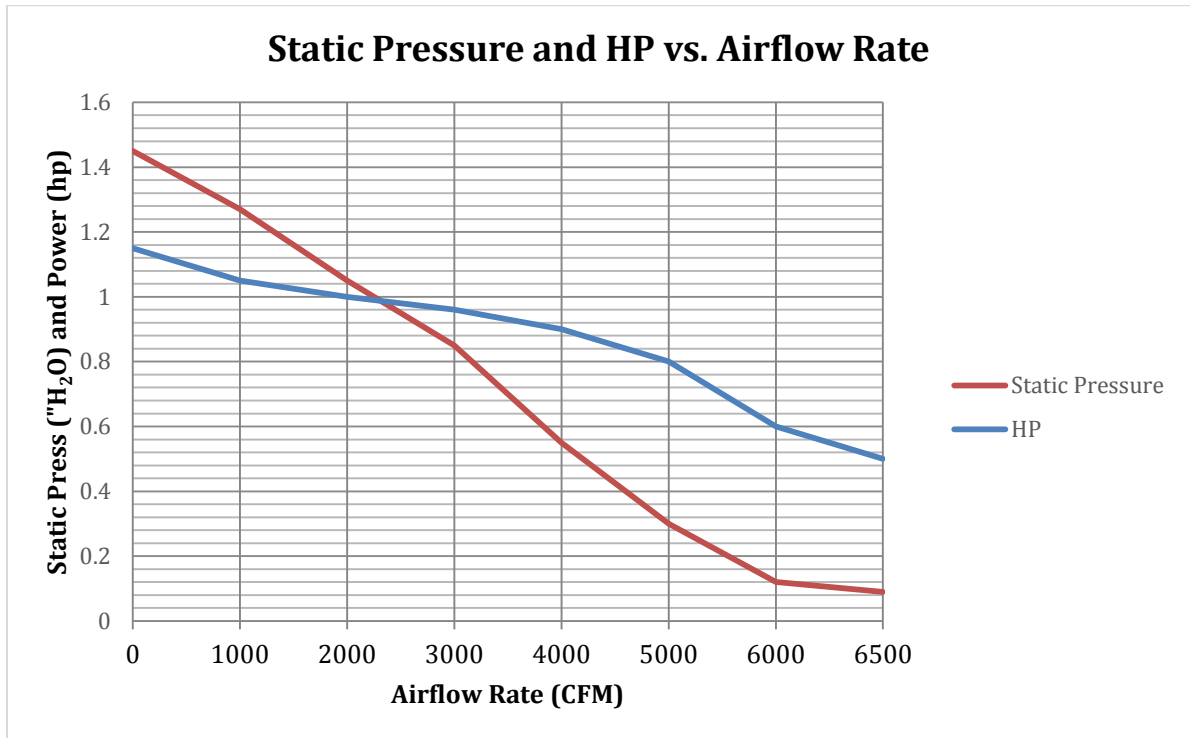


Figure 18: Fan Curve (Drake Refrigeration)

The fan curve shows that a lower pressure drop will allow more CFM to be pulled through the condenser coil. Fan blades can be used with a variety of motor horsepower for a variety of applications. For this chiller application at 5,500 cfm, the static pressure drop is 0.22 in-WG and the fan horsepower required is at least 0.70 hp. The blue plot shows the horsepower required, and in this case, the $\frac{3}{4}$ hp fan motor will be required as it sits above the next smallest common motor size of 0.5 hp. The air flow rate is able to follow the static pressure plot if the condenser coil causes less static pressure than the plot and has a fan motor greater than the required horsepower in the blue plot. As one can see from Figure 18, more condenser fan power would be required for more than 0.25" WG. At a static pressure of 0.30 "WG the fan blade requires a 0.80 hp motor. The next common motor size above 0.75 hp is the 1.0 hp, which is not part of our standard product. The desire is to use one fan motor across the product line for familiarity and pricing discount based on a current quantity purchased. Therefore, the condenser coil will need to be selected with a pressure drop of below 0.25 in. WG to make this chiller a cost effective addition to the chiller product line.

Based on the simulation of all the different area coils, optimum operating parameters were found. An optimum subcooling of 5 F was selected for use in order to ensure the unit is not undercharged, while not sacrificing efficiency. An optimum volumetric flow rate of 11,000 cfm was chosen based on the effectiveness of this air flowrate and being able to use the current fan motor and blade assembly. The optimum air velocity of 10.5 ft/s was chosen to ensure that heat would be removed at a serviceable rate while minimizing the pressure drop through the coil. These optimum operating parameters were selected to narrow down the possible condenser coils that were simulated. Each condenser was considered at these optimum parameters in addition to the constraints from the overall size and air pressure drop. The maximum allowable length of the chiller is 85 in. long and in order to be able to mount the condenser coil with support at the corners, the coil would need to be shorter than this length. The condenser coil also needed to be long enough in order for two fan blades to be able to evenly pull air through the system. Due to these constraints the frontal area condenser that will be further investigated using the optimum conditions is a condenser coil 75" long x 36" tall with varying rows.

Once the condenser coil of 75" x 36" was selected, it enabled a more in depth study using the optimization parameters. The number of rows of this condenser coil was varied in order to optimize the overall area required for this chiller. The number of rows was varied from 3-6 rows to focus on the effect on the overall coil performance. Air pressure drop was the first variable investigated as shown below in Figure 19: "Air Pressure Drop vs. Rows". As was shown in the previous discussion as the number of rows increased, the air pressure drop also increased. In this plot the static pressure increases from 0.17 in-wg at three rows up to 0.33 in-wg at 6 rows. Based on the fan curve above, (Figure 18), in order to be able to move 5,500 cfm the static pressure restriction can only be 0.23 in-wg. The simulated condenser coil with 4 rows only has a static pressure drop of 0.22 in-wg. By using the 4-row coil, this would enable the use of the current existing fan motor and blade assembly. Based simply on air pressure drop the 4 row condenser coil would be the optimized choice. However, there are other factors to consider and they are investigated now.

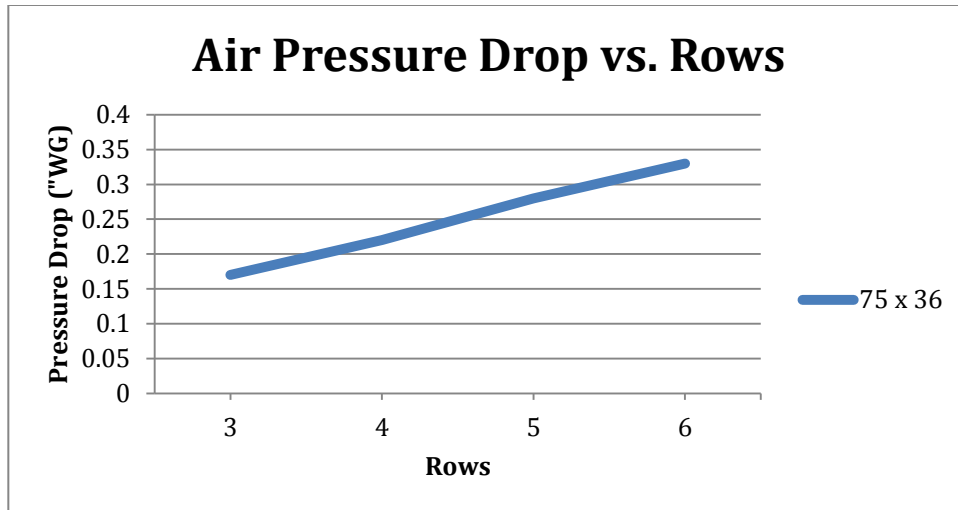


Figure 19: Air Pressure Drop vs. Rows

The next parameter that will be evaluated is the effect of varying the quantity of rows will have on the saturated condensing temperature. The saturated condensing temperature is a direct indication of how effectively the coil can remove excess heat from the refrigerant cycle. The lower the condensing temperature the lower the power consumption of the compressor to produce the same capacity. As shown in Figure 20: “Saturated Condensing Temperature vs. Rows” there is a downward slope in the condensing temperature as the number of rows increase. For the 3 row coil the saturated condensing temperature is at 128.4 F, while the 6 row coil yields a condensing temperature of 115.3 F. The local ambient design temperature near Philadelphia is 95 F and this is used in this study. As mentioned earlier in this report, the temperature difference from ambient to condensing temperature is desired to be between 20-30 F. This temperature difference is not affected by ambient changes. If there is an increase in the ambient temperature, there will also be an increase in the condensing temperature, but the TD will remain constant. However, as the ambient temperature rises, less heat can be rejected from the condenser coil due to the hotter ambient. This will cause the condenser to operate at an elevated condensing temperature due to the elevated ambient.

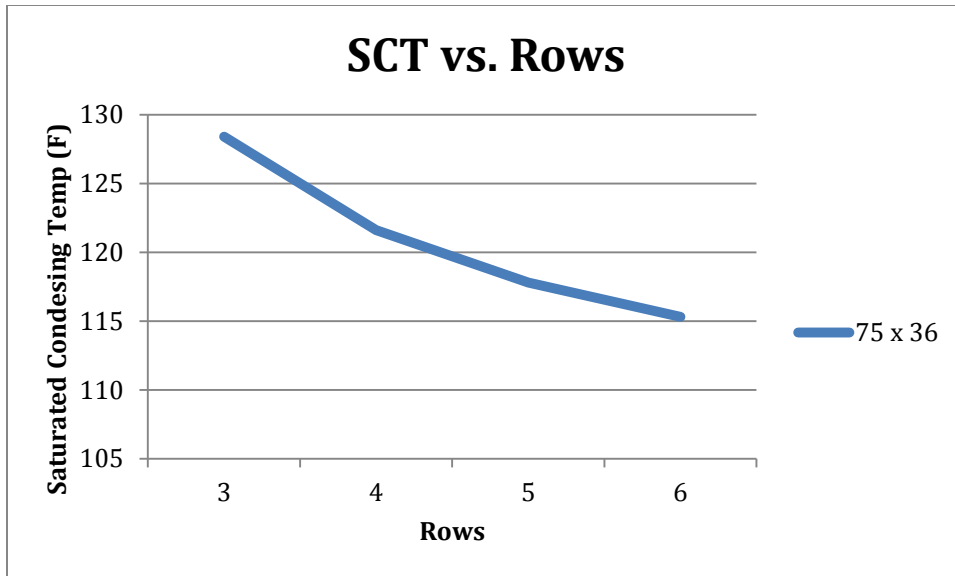


Figure 20: Saturated Condensing Temperature vs. Rows

Because the condensing temperature increases with higher ambient temperature, the compressor works harder to produce the same capacity. This causes the efficiency of the unit to decrease with the increasing ambient temperature. This is reflected in Figure 21: “EER vs. Rows” where the efficiency of the chiller increases as the number of rows increases on the condenser coil. This plot has an upward slope that is a direct inverse of the “Saturated Condensing Temperature vs. Rows” plot in Figure 20. The saturated condensing temperature has a direct effect on the efficiency of the chiller operation. The lower the condensing temperature, the more efficient the chiller will operate.

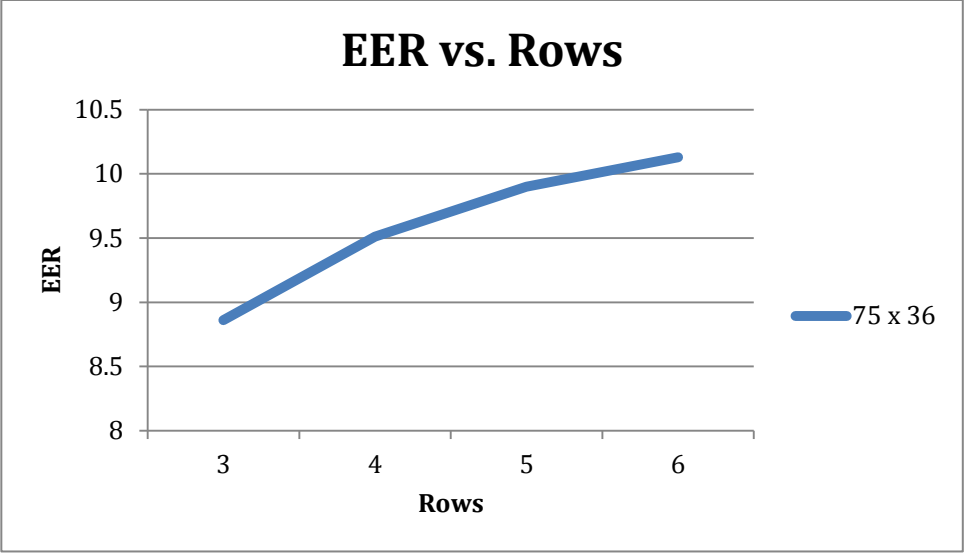


Figure 21: EER vs. Rows

Keeping the compressor operating at lower temperatures will keep the efficiency of the system higher and keep the yearly operating cost of the chiller down. A yearly operating cost was calculated using the power consumption at an average rate of \$0.10/KWh in the Philadelphia area. This took into consideration the seasonal temperature swings and using the chiller year round for a industrial process application. This is shown in Figure 22: “Yearly Operating Cost vs. Rows”.

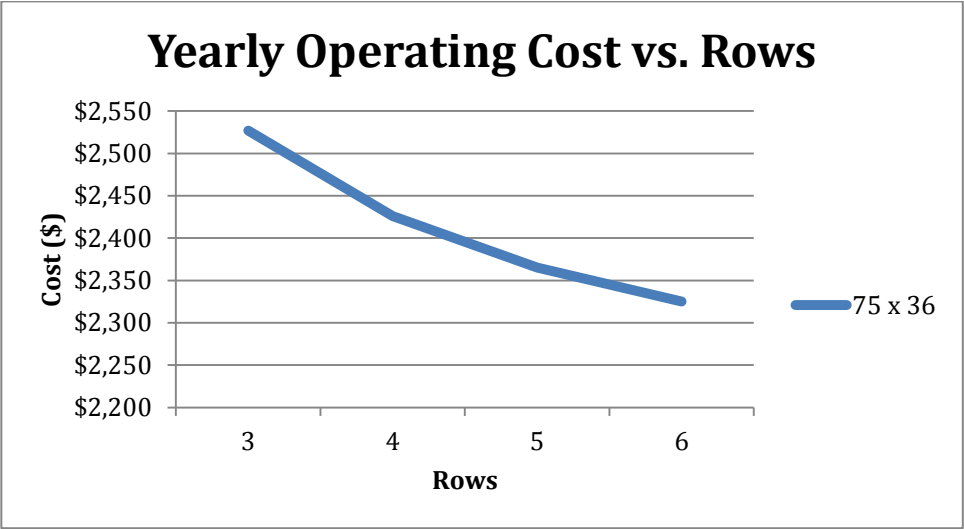


Figure 22: Yearly Operating Cost vs. Rows

The savings generated by increasing the number of rows starts at \$100 per year when going from 3-4 rows and only a savings of \$40 per year when going from 5-6 rows. The operating cost for the condenser with 4 rows was \$2,426 and 5 rows was \$2,365, in order to run this chiller year round in Philadelphia. These costs are typical for this size of chiller in this region.

Chapter 6.1-Condenser Coil Selection

Two major restrictions on the condenser coils controlled the coil selection. The first constraint was the overall physical size of the chiller (85 in. long x 40 in. wide x 45 in. high). The second constraint was the desire to use the fan motor and blade assembly that is currently being used by the rest of the product line. The frontal area of 75 in. x 36 in. was chosen based on chiller size. This led to a closer study of the effect the number of rows has on performance. The condenser frontal area remained constant while the number of rows was varied from 3 to 6. The saturated condensing temperature decreased with the number of rows that were added to the coil. The goal is to have a TD of 20-30 F in order to keep the system running cooler and more efficient. This eliminated the use of the 3 rows immediately, as it had a TD of 33.4 F. The EER ratings for the condenser coil with 4 rows was 9.51, 5 rows was 9.9, and 6 rows was 10.13. These higher EER ratings translated into a lower operating costs where 4 rows cost \$2,426, 5 rows cost \$2,365, 6 rows cost \$2,325. The EER of the units increased with more rows and with corresponding lower operating annual costs. However, the difference in operating costs from 4 rows to 6 rows would not sway a designer to select one condenser over another.

The other major practical restriction is the desire to continue using the same $\frac{3}{4}$ hp fan motor and 24" four blade assembly. The consistency and availability across our product line for consumers of using one fan assembly simplifies the product line. In this study it was desired to move between 10,000 cfm to 12,800 cfm and in order to efficiently remove excess heat from the chiller system. This fan assembly is able to move 11,000 cfm at a static pressure less than 0.22 in-wg before requiring a larger horsepower motor. Therefore this fan assembly was chosen to be the operating point for the desired airflow. By selecting this volumetric flow rate, the coils produced the following: 4 rows-0.22in-wg, 5 rows-0.28in-wg, and 6 rows-0.33in-wg. These pressure drops allowed only the 75 in. x 36 in. x 4 rows coil to be the only condenser that could meet all the demands for the chiller.

The 75 in. x 36 in. x 4 rows coil maximizes the use of the chiller size along with allowing the continued use of the fan motor and blade assembly. A prototype condenser coil with these predicted optimized dimensions is being fabricated and will be experimentally evaluated.

Chapter 7 - Conclusions and Recommendations

7.1 Conclusions

While the primary objective of this study was to find the most energy efficient chiller system by optimizing the condenser coil, the system constraints must also be considered when detailing the selection of the optimized design. This includes the physical restrictions limiting the overall size of the unit and the use of the already selected fan motor and blade assembly. It is concluded that the selection of the final optimum configuration depends on the constraints imposed by the system designer. If there are no space constraints and a higher EER is the primary goal, then the condenser configuration for the system would have been different.

From this investigation, it is concluded that:

- + Condenser designs for chiller systems must be based on energy efficiency ratings in order to allow for a comparison between two chillers.
- + When chiller space constraints are not restrictive, the condenser configuration with the largest frontal area yields the best system performance.
- + Condenser tubes with smaller diameters enhance performance. In this study 5/16 in. tubes were used, as they are common in industrial process water chillers.
- + Altering the fin density, FPI, only adjusts the overall system performance, or EER, by 5%.
- + Operating parameters of a chiller can drastically alter the system's performance and condenser coil that is required. For example, a nominal 12.5-ton chiller at 45 F leaving fluid temperature will only provide 7 tons at 10 F leaving fluid temperature.
- + For all condenser configurations simulated, a refrigerant charge yielding between 5-10 F subcooling at 95 F ambient temperature produces the optimum performance as indicated by the EER.

- + For all condenser configurations investigated, the optimum air velocity over the condenser coils range between 8 ft/s to 10.5 ft/s. This velocity range yielded acceptable air pressure drops in conjunction with constraints while still allowing sufficient heat exchange.
- + For all condenser configurations simulated, the optimum volumetric airflow range through the condenser coils is between 10,000 to 12,800 cfm.
- + Increasing the number of rows in a condenser coil has a diminishing effect on performance of the coil with greater than 7 rows.
- + For each row that is added to the condenser coil, an increased pressure drop of 0.06 in-wg occurs for air traveling between 8-12 ft/s.
- + Increasing the airflow by 2,000 cfm caused an increase in system efficiency EER by 0.3.
- + For all coil sizes studied, the refrigerant charge that produces a subcooling between 5-15 F only decreases the EER by 0.03. Therefore, it is safer to charge the unit to the point where there is enough subcooling to ensure maximum output from the system while sacrificing minimal efficiency.

7.2 Recommendations

After completing this study on the new coils built with a standard platform from the coil manufacturers, further investigation is recommended regarding condenser coil tube size and spacing. Specifically: diameter of the tubes, thickness of the tube walls, and horizontal tube spacing.

- + When designing a new condenser coil, decreasing the temperature that the system condenses at will help increase overall system efficiency.

- + Evaluate the effect of varying the condenser tube circuiting. This would add no cost to the system but may drastically improve the performance of the condenser.

- + The spacing of the tubes in the condenser during this investigation is the standard spacing provided by most coil manufacturers. However, it is possible that different spacing may yield an optimum coil and this should be evaluated.

- + In this study, the sizes of the tubes in the condenser were 3/8 in. od. This size is the commercial process industry standard used by most coil manufacturers. Smaller tubes may yield higher efficiency and should be evaluated.

- + Currently, the EPA program Significant New Alternative Policy (SNAP) was approved at the end of September 2016 that eliminates the use of many common refrigerants by 2024 including: R404a, R407c, R410, due to their higher GWP ratings. Therefore, condenser optimization studies will have to be done in the coming years for the new environmentally friendly refrigerants.

- + After completing this study where optimizing the size of the condenser was the primary objective, this study could be redone to optimize condenser cost alone or chiller system cost.

- + Varying the fan motor and blade assembly would eliminate a constraint in optimizing the system. Not being tied to a specific fan model would allow optimization of any frontal area and number of rows in a condenser coil. This should be investigated in future studies.

Chapter 8 - References

1. AKAspelund, K. A. (2001, December 1). OPTIMIZATION OF PLATE-FIN-AND-TUBE CONDENSER PERFORMANCE AND DESIGN FOR REFRIGERANT R-410A AIR-CONDITIONER. Retrieved February 5, 2016, from <http://citeseerx.ist.psu.edu/viewdoc/download?doi=10.1.1.148.4062&rep=rep1&type=pdf>
2. Jacobi, A. M. (2006, March 2). Heat Transfer to Air Cooled Heat Exchangers. Retrieved January 1, 2016, from <http://www.wlv.com/wp-content/uploads/2014/06/data/db3ch6.pdf>
3. Bergman, T. L., Lavine, A. S., Incropera, F. P., & Dewitt, D. P. (2011). *Fundamentals of Heat and Mass Transfer* (7th ed.). Hoboken, NJ: John Wiley and Sons Inc.
4. Rich, D. G., "The Effect of Fin Spacing on the Heat Transfer and Friction Performance of Multi-Row, Smooth Plate Fin-and-Tube Heat Exchangers," *ASHRAE Transactions*, vol. 79, pt. 2, pp. 137-145, 1973.
5. McQuiston, F. C. and Parker, J. P., *Heating Ventilating and Air-Conditioning-Analysis and Design*, John Wiley & Sons, New York, 1994.
6. Drake Refrigeration, "Drake Chillers- The Leaders in the Chiller Industry", Drake Refrigeration company website, <http://www.drakechillers.com/>, Accessed March 2016.